Chemical Geology 414 (2015) 42–58

Contents lists available at ScienceDirect

Chemical Geology

journal homepage: www.elsevier.com/locate/chemgeo

Effect of the volcanic front migration on helium, nitrogen, argon, and carbon geochemistry of hydrothermal/magmatic fluids from Hokkaido volcanoes, Japan

Emilie Roulleau [a,b,*], Nicolas Vinet [b,c], Yuji Sano [a], Naoto Takahata [a], Hiroshi Shinohara [c], Mitsuhiro Ooki [a], Hiroshi A. Takahashi [c], Ryuta Furukawa [c]

[a] The University of Tokyo, Atmosphere and Ocean Research Institute, Kashiwa, Japan
[b] Andean Geothermal Centre of Excellence (CEGA) and Department of Geology, Universidad de Chile, Santiago, Chile
[c] Geological Survey of Japan, AIST, Tsukuba, Japan

ARTICLE INFO

Article history:
Received 17 December 2014
Received in revised form 6 August 2015
Accepted 9 August 2015
Available online 31 August 2015

Keywords:
Hokkaido volcanoes
Helium
Nitrogen/argon
Carbon
Recycling of volatiles

ABSTRACT

Active volcanoes from Hokkaido are distributed along the SW–NE trending volcanic front, where the subducting Pacific plate changes direction from N–S to WSW–ESE. One exception is the Tokachi volcano, which is located approximately 50 km to the north-west of the current volcanic front. The Tokachi–Oki slab cracking zone represents the transitional zone between the Honshu and Kurile trenches. This change is responsible for the rapid lateral variation of the subduction angle and slab shape. We investigate the consequence of this change on the chemical and isotopic compositions from hydrothermal/magmatic fluids and mineral separates collected from three volcanoes of Hokkaido, northern Japan, namely Tarumae, Tokachi, and Meakan. Our data show that these volcanoes have a distinct range of He, N, and C isotopic compositions. Meakan fumaroles have a $^3He/^4He$ ratio that ranges from 4.46Ra to 6.88Ra, $\delta^{15}N$ from +2.2‰ to +3.5‰, and $\delta^{13}C$–CO_2 from −8.47‰ to −9.81‰, consistent with subducted sediment contribution. Tarumae fumaroles have a particularly low $^3He/^4He$ ratio (3.08Ra) in comparison with their hot springs (up to 5.24Ra), and are associated with high $CO_2/^3He$ ratios ($2.2–5.3 \times 10^{11}$). Hydrothermal–crustal interactions, from the dome or from a deeper hydrothermal system, are the main mechanisms that control the $^3He/^4He$ (and $CO_2/^3He$) ratios in Tarumae fumaroles. The $\delta^{15}N$ and $\delta^{13}C$–CO_2 values for Tarumae volcano range from −0.6‰ to 3.1‰ and from −6.34‰ to −6.43‰, respectively. Tokachi fumaroles are characterized by high $^3He/^4He$ (up to 7.38Ra), low $\delta^{15}N$ (−2.4‰–0.1‰), and low $\delta^{13}C$–CO_2 (up to −5.32‰), consistent with mantle contribution and minor subducted sediment contribution. The (Limestone + Sediment)/Mantle ratio shows a decreasing contribution from subducted sediments starting from Tokachi (1.9), to Meakan (3.4) and finally Tarumae (5.3). This change of isotopic compositions from the SW–NE of Hokkaido is the result of the Tokachi-Oki slab cracking zone. Slab dehydration under Tokachi occurs at a deeper level (150–200 km) than in other Hokkaido volcanoes (100 km), which produces the migration of the volcanic front. Therefore, we argue that the isotopic signature of Tokachi is the result of (i) a lower sediment contribution from the slab, (ii) a deeper dehydration of the slab, and (iii) a lower degree of partial melting.

1. Introduction

Determination of noble gases (i.e., He, Ar) and stable isotope (i.e., C and N) compositions from fumarole and hot spring fluids in arc settings is used to identify the contribution of different reservoirs. These can be the mantle wedge, subducted slab or sediments, and/or air in the formation of arc magmas (Hilton et al., 2002; Ozima and Podosek, 2002). Nitrogen and carbon are excellent tracers to identify and quantify subducted slab and sediment contribution from subduction recycling, while helium is more useful for tracing mantle contributions (Sano and Marty, 1995; Sano et al., 2001; Fischer et al., 2002).

To better understand the cycle of nitrogen and carbon in a subduction zone, we focused our research on the Hokkaido volcanic arc, Japan. Hokkaido is located where the Pacific plate changes from a N–S direction along the Honshu trench, to a SW–NE direction along the Kuril trench. At this location, the dip of the subduction slab also increases from south to north (Wang and Zhao, 2005).

All active volcanoes in Hokkaido such as the Usu, Tarumae, and Meakan volcanoes are located along the volcanic front. One exception is the Tokachi volcano, which is located at the rear arc, about 50 km to the north-west of the current volcanic front (Katsui, 1961; Ikeda et al., 1987). The model of detailed geometry of deep seismic zone, based on

* Corresponding author at: Andean Geothermal Centre of Excellence (CEGA), Department of Geology, Universidad de Chile, Plaza Ercilla 803, Santiago, Chile.
E-mail address: eroulleau@ing.uchile.cl (E. Roulleau).

http://dx.doi.org/10.1016/j.chemgeo.2015.08.006
0009-2541/

relocated hypocenters, showed that the Tokachi area is characterized by slab-cracking, torn by the extensional stress due to the rapid lateral change in dip of the subducting plate (Katsumata et al., 2003). This zone, known as the Tokachi-Oki slab-cracking zone is located under the Tokachi volcano, at the transitional point between the Honshu and Kurile trenches.

Previous geochemical and isotopic studies on the North Honshu and Kurile trenches show that K_2O content increases from the volcanic front (Tarumae, Meakan, Usu) to the rear arc (Tokachi). Meanwhile, Sr isotope ratios decrease, suggesting a lower degree of partial melting and a lower contribution of marine sediments in the magmas (Katsui, 1961; Katsui et al., 1978; Ikeda et al., 1987; Nakagawa, 1992; Kurima and Yoshida, 2006). Kurima and Yoshida (2006) presented a schematic model of magma genesis for the northern Honshu trench. These authors proposed that the chemical and isotopic variations with distance from the volcanic front are also the result of a low contribution of the dehydrated slab fluids. The particular chemical and isotopic composition of the Tokachi volcano compared to other active volcanoes in Hokkaido (from the volcanic front) suggests a different magmatic source. This is possibly related to different contributions from the mantle wedge and the subducted slab.

In this article, we present a detailed study on hydrothermal fluids from fumaroles, hot springs and bubble gases along the North Honshu–Kurile trench. The Tarumae, Tokachi, and Meakan volcanoes are among the most active in Hokkaido, and are considered representative of the volcanic activity on this island arc. The purpose of our research is to identify and characterize the main reservoir(s) that contributes to the volatile output emitted along the volcanic arc, particularly for these three volcanoes. We will also define the relationship between the volatile output and the particular geological setting.

2. Geological setting

Japan is located at the junction of four plates (North American, Pacific, Philippine and Eurasian plates) that produce a complex subduction setting. Hokkaido is the northernmost island of Japan, and is scattered with numerous active and inactive volcanoes. The curvature of the volcanic front is defined by the direction of the Pacific Plate, which changes from N–S along the Honshu trench (southwestern Hokkaido) to WSW–ENE along the Kurile Trench (northeastern Hokkaido) (Fig. 1A). At the Kurile and Honshu arc, the Pacific plate motion is ~8–9 cm/year and its age has been determined between 110 Ma and 130 Ma (Syracuse and Abers, 2006; Dreyer et al., 2010). The Kurile and Honshu arc is considered to have a cold subduction geothermal structure (Syracuse and Abers, 2006; Syracuse et al., 2010). This means that the oceanic lithosphere, the cooler upper boundary of the Earth, descends into the mantle more rapidly than heat conduction warms the slab.

2.1. Tarumae volcano

The Tarumae volcano is located on the southeast rim of the Shikotsu caldera (southwestern Hokkaido) just at the northern end of the Honshu trench, where the direction of the volcanic front changes (Fig. 1B). The Shikotsu caldera is dated at 60 ka (Watanabe, 1993). Its basement consists of Miocene/Pliocene subaqueous volcanic and sedimentary rocks (Doi, 1957). Tarumae consists of a crater 1.5 km in diameter formed between 1667 and 1739, with an andesitic lava dome in its center, formed during the 1909 eruption. The dome is 450 m in diameter and 150 m in height, and persistently degasses through strong fumarolic activity in the summit area: a-crater and b-crater. Its last eruption occurred in 1981. In 2001 and 2003, the highest temperature of the crater occasionally reached over 600 °C, and sand and mud were emitted from the a-crater (Japan Meteorological Agency, 2005). Mori et al. (2006) presented SO_2 and CO_2 fluxes for Tarumae of 0.24 kg/s and 0.24 kg/s, respectively. These fluxes are extremely low compared to very active volcanoes in Japan, such as Miyakejima (80 kg/s). These low values are explained by the lack of open-vent degassing.

2.2. Tokachi volcano

The Tokachi volcano consists of a group of dominantly andesitic stratovolcanoes and lava domes arranged in a NE–SW orientation above a plateau of welded Pleistocene tuffs (Fig. 1C). During the 1926 eruption, its summit collapsed during a phreatic phase, causing infrastructure damages due to lahar flows. Its last eruption occurred in 1988–1989. The Tokachi-Oki earthquake (M8.0) was recorded in 2003. Studies show that this earthquake produced accelerated plate subduction, caused local concentration of strain and resulted in inland earthquakes in the Meakan Area (Heki and Mitsui, 2013; Ichihara et al., 2013). The measured SO_2 and CO_2 in 2003 from Tokachi are 2.4 kg/s and 3 kg/s, respectively.

2.3. Meakan volcano

Meakan-dake is an andesitic volcanic complex located on the western edge of the Akan caldera (northeastern Hokkaido; Fig. 1D). Three major stages of explosive eruptive activity at 12 ka, 9 ka, and 5 to 6 ka were associated with the generation of pyroclastic flows. Successive lava effusions have continued fitfully over the last few thousand years. Many eruptions were registered between 1955 and 1965. Minor phreatic eruptions occurred in 1996 and 1998 inside the Ponmachineshiri crater. In 2003, SO_2 and CO_2 flux was reported at 0.3 kg/s and 0.76 kg/s, respectively. The last eruption of Meakan occurred in 2008.

3. Samples and analytical methods

Seven high-and-low-temperature fumarole samples were collected from Tarumae (a- and b-craters), Tokachi (Taisho crater), and Meakan (Nakamachineshiri crater and northern flank of Akanuma crater; Table 1) volcanoes. Fumarole gases were sampled using a titanium tube connected by a silicone tube to a lead glass bottle and cold trap. The lead glass bottle and cold trap were plunged in a mixture of cold water and ice. We also collected five water samples from natural hot springs (*onsen*) and one bubbling gas sample from each of the Tarumae, Tokachi, and Meakan areas (Table 1). Water from natural hot springs was sampled in lead glass containers using a manual pump. Bubbling gas samples were sampled using a lead glass container with vacuum valves at both ends, following a water displacement method. Dissolved gases from water samples were then extracted in the lab using a glass bottle under vacuum, which was plugged to the extraction line. Gas samples were also collected into Pyrex flasks (Giggenbach bottles) containing 20 mL of 4 N NaOH solution for absorption of acid gas.

Olivine and clinopyroxene (1.5–2 g) from Tarumae pumice (AD 1739) were carefully selected and separated for He analyses. Mineral separates were ultrasonically cleaned in ultrapure water, ethanol and acetone for 20 min, dried overnight, and loaded in a ball mill-type crusher. The crusher is made of a stainless-steel cylinder containing a steel ball and is connected to an extraction line by a bellow. The crusher and the samples were baked at 100 °C overnight. Samples were manually crushed for 5 min. Helium was purified using a hot Ti-getter and a charcoal trap at the temperature of liquid nitrogen. The $^4He/^{20}Ne$ ratio was measured using an online quadrupole mass spectrometer. The detection limit for ^{20}Ne was 4.06×10^{-10} cm^3 STP. Helium was separated from Ne using a cryogenic trap held at 40 K (Sano and Wakita, 1988). The $^3He/^4He$ ratio was measured on a Helix mass spectrometer. Typical blank was 2.51×10^{-10} cm^3 STP for ^4He and 2.85×10^{-16} cm^3 STP for ^3He.

Nitrogen isotopic analyses were carried out at the Atmosphere and Ocean Research Institute (AORI), University of Tokyo, Japan. The

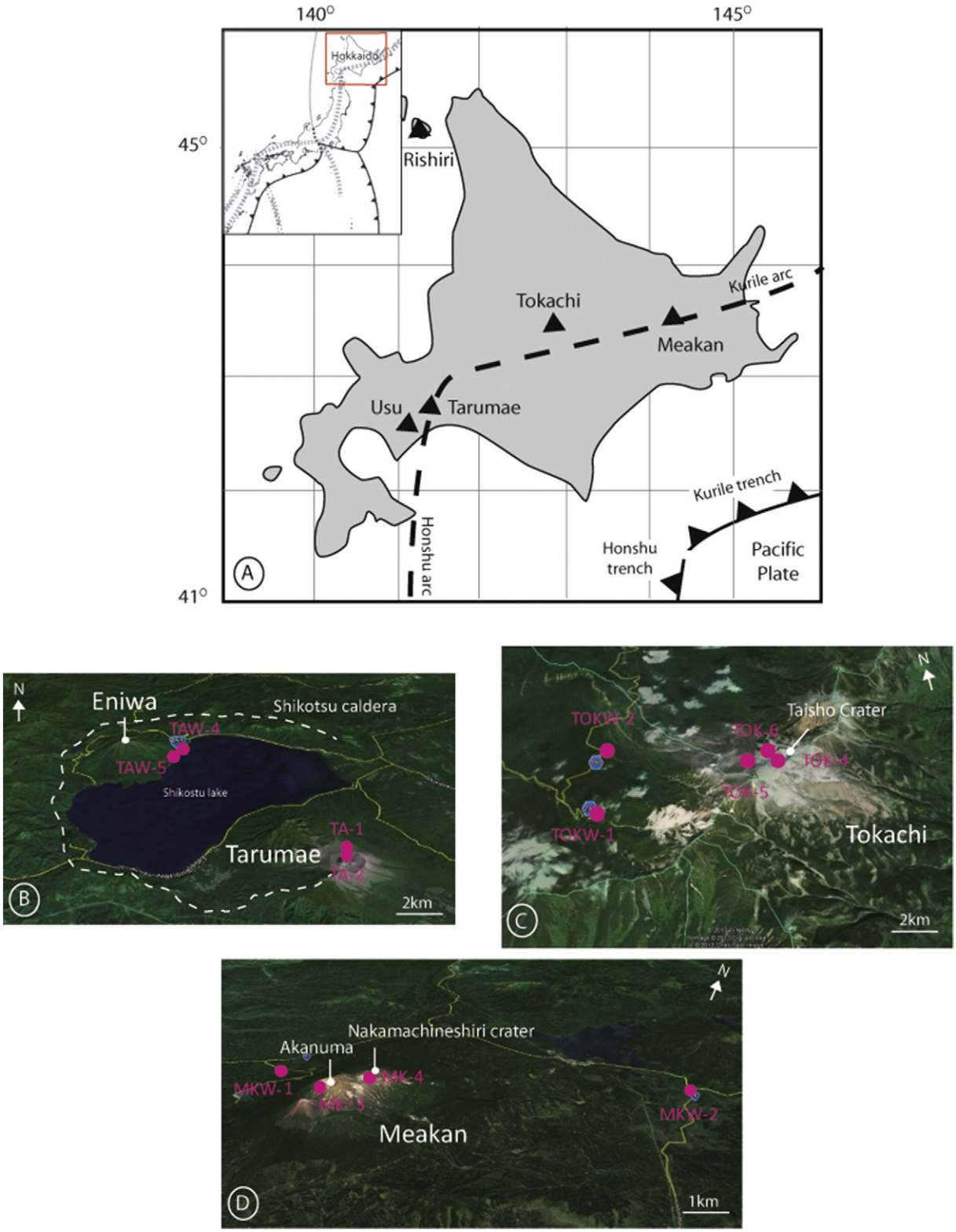

Fig. 1. A) Location of Tarumae, Meakan and Tokachi volcanoes, Hokkaido, Japan. The volcanic front is illustrated by a dotted line, and the volcanic trench is illustrated by a solid line with a triangle. The Google Earth images are presented for each volcano, B) Tarumae, C) Tokachi and D) Meakan, to locate the fumarole, water and bubbling gas samples.

measurements were done on a static magnetic-sector mass spectrometer VG3600, equipped with Faraday cups and calibrated against a purified atmospheric N standard. Details regarding the extraction procedures and general performance of the instruments are presented in Takahata et al. (1998).

The nitrogen isotopic composition is given by the equation:

$$\delta^{15}N = \left(\left[{}^{15}N/{}^{14}N \right]_{sample} \Big/ \left[{}^{15}N/{}^{14}N \right]_{air} - 1 \right) \times 1000 \quad (1)$$

Table 1
Chemical and isotopic compositions of hot springs, bubbling gas and fumaroles at Tarumae, Tokachi and Meakan.

Name	Location	Type	Distance from the crater (km)	Latitude (DMS)	Longitude (DMS)	Temperature (°C)	$^4He/^{20}Ne$	$^3He/^4He$ R/Ra	±	$^3He/^4He$ Rc/Ra	±	N_2/Ar	±	$\delta^{15}N$	±
TAW-4	Ito Onsen (Tarumae area)	Hot spring	11.2	42,782	141,313	50	2.179	5.24	0.06	5.77	0.06	41.84	1.3	2.1	0.7
TAW-5	Marukoma (Tarumae area)	Hot spring	11.2	42,780	141,311	50	1.215	4.68	0.05	5.59	0.06	45.66	1.4	1.6	0.7
TA-2	b-crater (Tarumae)	Fumaroles	0	42,689	141,376	487	13.197	3.08	0.09	3.11	0.09	212.02	6.4	3.1	0.7
TA-1	a-crater (Tarumae)	Fumaroles	0	42,688	141,378	593	9.545	3.02	0.09	3.07	0.09	171.32	5.1	−0.6	1.1
TOKW-1	Tokachi SPA (Tokachi area)	Hot spring	4.17	43,415	142,642	45	0.346	1.83	0.04	3.71	0.19	41.89	1.3	2.1	0.7
TOKW-2	Fukiage onsen (Tokachi area)	Hot spring	4.33	43,431	142,641	40	0.315	1.79	0.04	4.35	0.31	64.50	1.4	7.2	0.8
TOK-4	Taisho (Tokachi)	Fumaroles	0	43,423	142,696	97	2.625	5.70	0.06	6.17	0.06	82.56	2.5	−2.4	0.7
TOK-5	Taisho (Tokachi)	Fumaroles	0.29	43,420	142,691	93	0.968	5.30	0.16	6.73	0.16	–		–	
TOK-6	Taisho (Tokachi)	Fumaroles	0	43,424	142,695	245	97.989	7.37	0.22	7.38	0.22	90.89	2.7	0.1	0.9
MKW-2	Oakan Onsen (Meakan area)	Bubbling gas	7.13	43,447	144,021	55	4.710	6.60	0.07	6.90	0.07	46.59	1.4	−2.6	1.1
MKW-1	Nonakan Onsen (Meakan area)	Hot spring	2.8	43,395	143,983	43.2	3.940	6.04	0.08	6.37	0.08	71.58	2.2	4.9	0.7
MK-4	North Flank (Meakan)	Fumaroles	0	43,386	144,001	240	33.503	6.88	0.07	6.92	0.07	128.25	3.9	3.5	0.7
MK-3	Nakamachineshiri crater (Meakan)	Fumaroles	0.2	43,390	144,017	94.5	0.645	4.46	0.13	6.53	0.15	85.43	2.6	2.2	0.7

Note: * These data are measured using a gas chromatographer from AIST, Japan. The errors for R/Ra and Rc/Ra are estimated at 1 σ.

Table 1 (*continued*)

Name	$^{40}Ar/^{36}Ar$	±	$N_2/^{36}Ar$	±	$\delta^{13}C$–CO_2	±	$CO_2/^3He$ (∗10^9)	He/Ar	N_2/He (∗10^2)	He (ppm)	CH_4 (%)	N_2 (%)	O_2 (%)	Ar (%)	H_2S (%)	CO_2 (%)	SO_2 (%)
TAW-4	–		–		−11.86	0.24	10.7	0.003	186.54	10.44	0.0	19.48	0.0	0.37	0.0	81.70	0.0
TAW-5	–		–		−11.37	0.07	11.1	0.002	298.80	9.90	0.0	29.57	0.0	0.58	0.03	71.97	0.01
TA-2	323.7	9.7	68,629	2117	−6.34	0.10	218.0[a]	0.019[a]	118.89[a]	–	–	–	–	–	–	–	–
TA-1	318.4	9.6	54,552	1773	−6.43	0.05	535.6[a]	0.014[a]	503.43[a]	–	–	–	–	–	–	–	–
TOKW-1	–		–		−7.05	0.08	44.5	0.001	319.56	6.91	0.0	22.09	0.0	0.46	0.0	78.57	0.01
TOKW-2	–		–		−7.11	0.06	53.6	0.001	640.48	4.96	0.0	31.79	1.05	0.49	0.01	66.65	0.0
TOK-4	291.9	8.8	24,095	723	−5.23	0.08	7.0	0.007	148.67	13.72	0.0	20.40	2.81	0.20	0.0	76.50	0.10
TOK-5	–		–		–		4.9	0.003	318.52	13.70	0.0	43.64	5.93	0.43	0.0	50.00	0.01
TOK-6	296.6	8.9	26,981	842	−5.32	0.04	2.1	0.420	3.89	42.92	0.0	1.67	0.0	0.01	0.01	93.71	5.44
MKW-2	319.9	9.6	14,906	447	−7.86	0.03	5.4	0.002	268.1	12.92	0.55	34.64	0.0	0.62	0.0	64.63	0.0
MKW-1	–		–		−9.43	0.16	119.6	0.003	278.58	0.92	0.32	2.57	0.06	0.03	3.93	93.17	0.05
MK-4	294.0	8.8	37,710	1134	−8.47	0.15	9.8	2191	26.43	9.49	0.45	2.51	0.0	0.0	7.98	89.54	0.11
MK-3	–		–		−9.81	0.17	16.2	0.003	416.48	6.66	1.53	27.75	2.49	0.26	0.58	67.54	0.03

Mass static blanks are 6×10^{-12} for $^{28}N_2$ and 7×10^{-15} for $^{29}N_2$, and lack any significant effect on measurements of the nitrogen isotopic ratios (0.1%). The error in the $\delta^{15}N$ values reported in Table 1 is the propagated error in the isotopic measurement of N for the sample and the standard, assumed at 1σ. After nitrogen isotope measurements, the $^{28}N_2/^{40}Ar$ ratio was determined by measuring the $28^+/40^+$ ratio using the same mass spectrometer and calibrated against air standard, with an error assumed at 1σ.

Argon isotopic analyses were also performed at AORI. The $^{40}Ar/^{36}Ar$ ratio was measured using an online quadrupole mass spectrometer (Massmate100, ULVAC Co.), after purification using a hot Ti-getter. The measurement error was 1–2% at 1σ.

The $^3He/^4He$ ratio was measured on a conventional noble gas mass spectrometer (Helix-SFT and VG-5400) at AORI. The $^4He/^{20}Ne$ ratio was measured using an online quadrupole mass spectrometer. Helium was separated from Ne using a cryogenic trap held at 40 K (Sano and Wakita, 1988). The observed $^3He/^4He$ ratio was calibrated against atmospheric helium. Experimental errors for $^4He/^{20}Ne$ and $^3He/^4He$ ratios were about 5% and 1% at 1σ with the Helix spectrometer, and about 5% and 3.5% at 1σ with the VG5400 spectrometer, respectively (Sano et al., 2008). The $^3He/^4He$ ratio was corrected for the presence of atmospheric He, using the He/Ne ratio of the sample (Craig et al., 1978). It is assumed that Ne in magmatic and crustal gases is negligible, and that essentially all Ne in geothermal gas samples is atmospheric. Accordingly:

$$Rc/Ra = \left(\left(^3He/^4He\right)_{obs} - r\right)/(1-r) \quad (2)$$

$$r = \left(^4He/^{20}Ne\right)_{ASW} \Big/ \left(^4He/^{20}Ne\right)_{obs} \quad (3)$$

where Rc/Ra and $(^3He/^4He)_{obs}$ denote the air-corrected and observed $^3He/^4He$ ratios, respectively, and $(^4He/^{20}Ne)_{ASW}$ and $(^4He/^{20}Ne)_{obs}$ are the ASW and observed $^4He/^{20}Ne$ ratios, respectively. The $(^4He/^{20}Ne)_{ASW}$ is 0.241 at 0 °C. The total error of the corrected $^3He/^4He$ ratio is defined in Sano et al. (2006). The error assigned to the corrected $^3He/^4He$ ratio in Table 1 includes all possible $^3He/^4He$ errors.

The $\delta^{13}C$ values of CO_2 were measured by a continuous flow GC–IRMS system at the Geological Survey of Japan, National Institute of Advanced Industrial Science and Technology (AIST), Tsukuba. CO_2 was separated from the sample gas using a Carboxen GC capillary column at 50 °C with He carrier gas flowing at 4 mL/min. Three measurements were carried out for each sample, but only the average value is reported here.

The carbon isotopic composition was measured in CO_2 component and is given by:

$$\delta^{13}C = \left(\left[^{13}C/^{12}C\right]_{sample} \Big/ \left[^{13}C/^{12}C\right]_{STD} - 1\right) \times 1000. \quad (4)$$

The δ-notation of the isotopic values is conventionally represented with respect to Vienna PeeDee belemnite (VPDB). Measurement errors of $\delta^{13}C$ are better than ±0.1‰.

Gas composition was determined by comparing peak heights of the samples with those of standard gases, using a quadrupole mass spectrometer at AORI. Experimental errors were estimated to be about ±10% by repeated measurements of standard samples. The measured blank for each component was negligibly small compared to the sample signal. Only elemental ratios of CO_2/He, N_2/He and He/Ar are reported.

Gas compositions were determined by gas chromatography at the Geological Survey of Japan, AIST, Tsukuba. The CO_2 content was determined acidimetrically on the alkaline condensates as described by Giggenbach and Goguel (1989).

4. Results

Table 1 presents the chemical and He, N, Ar and C isotopic compositions of hot springs, bubbling gases, and fumaroles from Tarumae, Tokachi, and Meakan volcanoes. The CO_2/He, N_2/He, and He/Ar ratios reported for Tarumae fumaroles as well as He contents for each volcano are data from gas chromatography analyses. Gas composition for Tokachi volcano and for Tarumae a-crater and b-crater in 1992 (Scott et al., 1994) and 2012 (this study) are presented in Table 2.

4.1. Chemical compositions

With the exception of TOK-5, TOK-4 and MK-3 samples, O_2 concentrations were less than 1% (Table 1).

The N_2/Ar ratio of water-dissolved gases and bubbling gases from the three volcanoes ranged from 42 to 72. However, the N_2/Ar ratio of fumaroles had a higher range, from 91 to 212 (except for samples TOK-4 and MK-3, with values of 83 and 85, respectively).

The $CO_2/^3He$ ratios were calculated using CO_2/He and $^3He/^4He$ ratios for each sample. The $CO_2/^3He$ ratio for water-dissolved gases ranged between 1.06×10^{10} (Tarumae) and 1.18×10^{11} (Meakan), while bubbling and fumarole gases had values ranging from 2.12×10^9 (Meakan) to 5.36×10^{11} (Tarumae). These results were all higher than those observed for MORBs ($CO_2/^3He = 2 \pm 1 \times 10^9$; Marty and Tolstikhin, 1998). These results fall within the same order of magnitude or are higher as those observed in volcanic arcs.

The gas composition of Tarumae a-crater and b-crater, showed a high CH_4 and N_2 content, and a low-to-moderate SO_2, H_2S, and HCl content. This is opposite to the trend generally observed in volcanic gases (Giggenbach, 1992b), and opposite to Tokachi as well, where high contents of CO_2, SO_2, and HCl and low contents of N_2 and CH_4 have been reported. The SO_2/H_2S and CO_2/S ratios for Tarumae ranged from 0.5 to 0.8 and 5 to 11, respectively, while those of Tokachi were 3.3 and 1.6, respectively.

4.2. He, Ar, N, and C isotopes

The $^3He/^4He$ ratio normalized to the atmospheric ratio (Ra = 1.382×10^{-6}; Mabry et al., 2013) is presented together with $^4He/^{20}Ne$ ratios in Fig. 2. Tarumae volcano (Fig. 2A) showed moderate $^3He/^4He$ ratios for hot springs (4.73Ra to 5.29Ra). However, fumarole samples had low $^3He/^4He$ ratios (3.02Ra to 3.08Ra) associated with high $^4He/^{20}Ne$ ratios. For Tokachi volcano (Fig. 2B), the $^3He/^4He$ ratios increased from hot springs (1.79Ra–1.83Ra) to fumaroles (5.70Ra–7.37Ra). The $^4He/^{20}Ne$ ratios also increased from hot springs to fumaroles. The Meakan volcano (Fig. 2C) showed the same trend as Tokachi, where $^3He/^4He$ ratios were low in hot springs (4.46Ra), and high in bubbling gas and fumaroles (6.04Ra–6.88Ra). The Rc/Ra ratios of water-dissolved gases, bubbling gases, and fumaroles at Meakan were all similar (6.43Ra–6.99Ra). Our data were consistent with the Meakan data reported by Marty et al. (1989; fumarole Rc/Ra ratio of 6.35Ra) but differed from the Meakan bubbling gas results of 5.6Ra reported by Sano and Wakita (1988).

Tokachi samples showed a smaller Rc/Ra ratio in water-dissolved gases (3.77Ra–4.43Ra) compared to fumaroles (6.28Ra–7.38Ra). Previous Rc/Ra data for Tokachi fumaroles ranged from 5.7Ra to 7.14Ra (Nagao et al., 1981; Marty et al., 1989), whereas values of 2.04Ra–3.72Ra for hot springs were reported by Sano and Wakita (1988), are consistent with our results.

Water-dissolved gases from Tarumae had a Rc/Ra ratio of ~5.74Ra, which was higher than the fumarole value (~3.09Ra). This surprising finding is noteworthy because it is the opposite of results previously found for Japanese volcanoes (Ontake and Kusatsu-Shirane) (Sano et al., 1994, 1998a). In contrast, a previous study on the Tarumae volcano only reported one corrected value of 3.72Ra for hot springs (Sano and Wakita, 1988).

The $^{40}Ar/^{36}Ar$ ratio of bubbling gas and fumarole samples ranged between 291.9 ± 8.8 and 323.7 ± 9.7, respectively. These data are consistent with previous data on fumaroles (305; Nagao et al., 1981), as well as the mean $^{40}Ar/^{36}Ar$ ratio observed in Japan (304 ± 9; Hilton et al., 2002) and at other arc volcanoes (401 ± 278; Hilton et al., 2002).

Table 2
Gas composition (μmol/mol) from Tarumae and Tokachi volcanoes.

Date of sampling	H_2O	CO_2	S	H_2S	SO_2	HCl	HF	He	H_2	N_2	Ar	CH_4
TA-2 (b-crater)												
2012	979,139	16,451	3059	2062	997	315	109	0.02	510	3777	0.90	32
1992	966,000	18,300	–	8100	41,000	2500	102	–	140	810	–	0
TA-1 (a-crater)												
2012	981,663	15,252	1418	784	634	148	24	0.01	1135	339	0.47	12
Tokachi												
2012	943,290	32,813	20,315	4671	15,643	3294	40	0.64	8	231	1	0

Note: data for b-crater (1992) are from Scott et al., 1994.

Our results of $\delta^{15}N$ from Hokkaido volcanoes are within the accepted range for subduction zones (−3‰ to +6‰; Hilton et al., 2002). The Tarumae and Tokachi $\delta^{15}N$ values were higher for water-dissolved gases (+1.6 ± 0.7‰ to +2.1 ± 0.7‰; +2.1 ± 0.7‰ to +7.2 ± 0.8‰, respectively) than values for fumaroles samples (+3.1 ± 0.7‰ to −0.6 ± 1.1‰; −2.4 ± 0.7‰ to 0.1 ± 0.9‰, respectively). The Meakan $\delta^{15}N$ values were positive and quite constant for hot springs (+4.9 ± 0.7‰) and fumaroles (+2.2 ± 0.7‰ to +3.5 ± 0.7‰) but were negative for bubbling gas samples (−2.6 ± 1.1‰).

For Tarumae, Tokachi, and Meakan, $\delta^{13}C$–CO_2 values were lower in water-dissolved gases (up to −11.86 ± 0.24‰ at Tarumae, −7.05 ± 0.08‰ at Tokachi, and −9.81 ± 0.17‰ at Meakan) compared to fumaroles (up to −6.34 ± 0.10‰ at Tarumae, −5.23 ± 0.08‰ at Tokachi, and −7.86 ± 0.03‰ at Meakan). Our fumarole samples were in the range of the observed values of high temperature volcanic gases from subduction zones (−5.5 ± 2.2‰; Sano and Marty, 1995).

Tarumae olivine and clinopyroxene separates showed a variable $^3He/^4He$ Ra of 5.22Ra and 3.73Ra, respectively. The $^4He/^{20}Ne$ ratio was 0.535 for clinopyroxene separate. The $^4He/^{20}Ne$ ratio for olivine separate was unknown because the ^{20}Ne signal fell under the detection limit (Table 3). The olivine $^3He/^4He$ ratio was comparable to the Tarumae hot spring $^3He/^4He$ ratio (5.74Ra), whereas the clinopyroxene $^3He/^4He$ ratio was smaller. These two observations suggest that 1) olivine and clinopyroxene $^3He/^4He$ ratios reflect different processes, and 2) the olivine $^3He/^4He$ ratio appears more representative of a primitive magmatic source (Hilton et al., 1995; Gautheron and Moreira, 2002; Shaw et al., 2006).

5. Discussion

In the following section we assess which samples are representative of the magmatic source and which samples have been affected by air contamination, shallow crustal contamination, or elemental/isotopic fractionation.

5.1. Air contamination

Three low-temperature fumarole samples from Tokachi and Meakan (TOK-5, TOK-4, MK-3) with O_2 contents above 3% showed evidence of air contamination (Table 1), probably related to the sampling. The atmospheric contribution related to Air-Saturated Water (ASW) can also be identified using the relative contents of He, Ar, and N_2. Air and ASW have a distinct N_2/Ar (83.6 and 38, respectively), N_2/He (1.48×10^5 and 2.64×10^5, respectively) and He/Ar (5.61×10^{-4} and 1.46×10^{-4}; Taran, 2011). Arc-type gases are characterized by high N_2 contents, with N_2/Ar of 107–338, N_2/He of 800–10,000, and He/Ar of 0.025–0.4 (Giggenbach, 1992a; Giggenbach and Corrales, 1992; Giggenbach and Glover, 1992; Marty, 1995; Sano et al., 2001; Zimmer et al., 2004; Fischer et al., 2005). The N_2/Ar ratios of hot spring, bubbling gas and two fumarole samples (TOK-4 and MK-3) ranged between 42 and 85, suggesting that arc-like N_2 and Ar have been diluted by atmospheric N_2 and Ar from meteoric water circulation and/or air. In contrast, the N_2/Ar ratio of the other fumarole samples (TA-1, TA-2, TOK-6 and MK-4) ranged between 91 and 212, similar to those observed in volcanic arcs (Fischer et al., 2005). With the exception of two fumaroles, MK-4 (2.20) and TOK-6 (0.42), our samples displayed very low He/Ar ratios (<0.02) that appear consistent with arc-type gases. However, the high He/Ar value (2.20) of sample MK-4 is similar to the MORB reference value (1 to 5; Graham, 2002). The N_2/He results can be divided into two groups: Group 1, comprised of hot spring and bubbling gas samples plus some fumarole samples, ranging from 6.41×10^4 to 1.87×10^4. Group 2 only includes samples MK-4 and TOK-6, with values of 2.64×10^3 and 3.89×10^2, respectively. In summary, most of our samples showed an air component associated with the interaction of meteoric water (ASW) related to groundwater circulation in the hydrothermal system of the three volcanoes. In contrast, two samples, MK-4 (Meakan) and TOK-6 (Tokachi), appeared to have elemental ratios unaffected by ASW addition; and hence are more representative of the magmatic source.

5.2. Crustal contamination and elemental/isotopic fractionation

Helium isotopes, $CO_2/^3He$ ratios, and $\delta^{13}C$–CO_2 values are generally known to be influenced by gradual addition of radiogenic ^4He and CO_2 from crustal rocks with distance from the crater (Sano et al., 1998a; Barry et al., 2013), with $^3He/^4He$ and $\delta^{13}C$–CO_2 decreasing and $CO_2/^3He$ increasing with distance. However, in the case of dissolved gases from hot springs, high $CO_2/^3He$ ratios can also reflect the solubility difference between CO_2 and He (Marty et al., 1989; Sano et al., 1998a). Elemental fractionation can occur between He and CO_2 where CO_2 solubility is greater than He solubility. As fluids migrate away from areas of up-flow in shallow geothermal systems, helium is lost faster than CO_2. This fractionation process may result in $CO_2/^3He$ ratios similar to the ASW solubility ratio of 4.4×10^{12} (Giggenbach and Poreda, 1993). Typical $CO_2/^3He$ and $^3He/^4He$ values for MORBs are 1.5×10^9 and 8 ± 1Ra, respectively, and 1×10^{13} and 0.02Ra, respectively, for the crust (Marty et al., 1989; Sano and Marty, 1995). $\delta^{13}C$–CO_2 of the MORB component is −6.5 ± 2.5‰ (Sano and Marty, 1995; Sano and Williams, 1996), while $\delta^{13}C$–CO_2 of sediments varies between two major components (Hoefs, 2009): (1) organic sediments (−40‰ to −20‰), and (2) marine limestone (including slab carbonates) (0 ± 2‰). $CO_2/^3He$, Rc/Ra, $\delta^{13}C$–CO_2, and $\delta^{15}N$ data from Tarumae, Tokachi and Meakan volcanoes versus the distance from the crater are shown in Fig. 3a–d. For comparison, the volcanic arc average values for $CO_2/^3He$, Rc/Ra, $\delta^{13}C$–CO_2, and $\delta^{15}N$ are $1.5 \pm 1.1 \times 10^{10}$ (Sano and Williams, 1996), 4.96Ra to 8.1Ra (Poreda and Craig, 1989; Sano and Marty, 1995; Fourre et al., 2002), −5.5 ± 2.2‰ (Sano and Marty, 1995) and −3‰–+6‰ (Hilton et al., 2002), respectively.

The $CO_2/^3He$ ratio of Tokachi samples increased with distance from the crater (Fig. 3a), from 2.12×10^9 (fumaroles) to 5.3×10^{10} (hot springs), suggesting that Tokachi hot springs are affected by crustal CO_2 contamination (Sano et al., 1998a). Fig. 3b–c shows negative correlations between both Rc/Ra and $\delta^{13}C$–CO_2 with distance from the crater, again reflecting crustal contamination in hot spring samples. A decrease of $\delta^{13}C$–CO_2 (from −5.23‰ to −7.11‰) toward the organic sediments end-member (−40‰ to −20‰; Hoefs, 2009) with respect to distance from the crater indicates that organic sediments are the crustal contaminants. Water-dissolved gas samples (hot springs) from Tokachi had

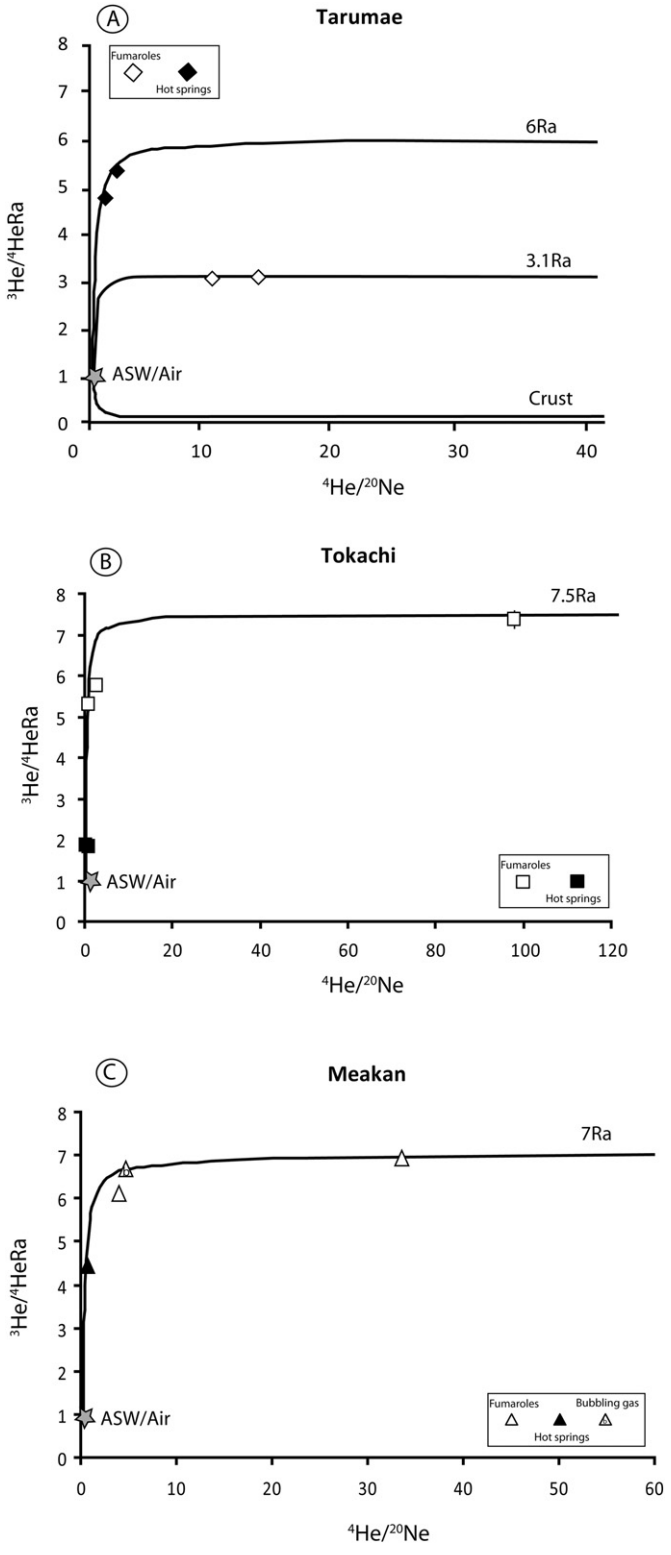

Fig. 2. ^{3}He/^{4}He Ra vs. ^{4}He/^{20}Ne ratios for (A) Tarumae, (B) Tokachi and (C) Meakan volcanoes. The solubility of He and Ne for ASW are calculated using a temperature of 0 °C and a salinity of 0‰. The ASW/Air–mantle and ASW/air–crust curves are from binary mixing models. The error is equivalent to the size of the symbols when not observable.

positive δ^{15}N (+2.1‰ to +7.2‰), while fumarole samples ranged between −2.4‰ and 0.1‰ (Fig. 3d). These results further support crustal fluid contamination of Tokachi hot springs related to water-rocks interaction.

Table 3
^{3}He/^{4}He ratios and He contents of olivine and clinopyroxene separate from Tarumae pumices.

Location	Mineral	Weight (g)	Date	^{4}He/^{20}Ne	^{3}He/^{4}He R/Ra	±	cm^{3}STP/g ($\times 10^{-9}$)
Tarumae	Olivine	1.5	1739	n.d.[a]	5.22	0.19	0.97
Tarumae	Clinopyroxene	1.8	1739	0.535	3.73	0.13	1.5

Note:
[a] It was not possible to determine ^{4}He/^{20}Ne ratio for olivine separate because the signal of ^{20}Ne was under the detection limit (4.06×10^{-10} cm^{3}STP).

Meakan fumarole and hot spring samples showed the same trend as Tokachi samples but were less pronounced. $CO_2/^3$He ratios increased (up to 1.18×10^{11}), Rc/Ra ratios decreased, δ^{15}N values increased (up to +4.9‰) and δ^{13}C–CO_2 values were similar (up to −9.43‰), with distance from the crater, again supporting crustal fluid contamination in hot spring samples. The bubbling gas sample (MKW-2) from Meakan had a similar $CO_2/^3$He ratio (5.38×10^9) as the fumaroles, suggesting that, although this sample was far from the active crater, no elemental fractionation or crustal fluid contamination had altered the volcanic gas composition, preserving a magmatic signature. This interpretation is supported by the high Ra/Rc ratio (6.97Ra), and comparatively high δ^{13}C–CO_2 value of MKW-2 (−7.86‰), again similar to the MK-4 fumarole sample (6.99Ra and −8.47‰ respectively; Fig. 3b, c). Bubbling gas sample MKW-2, which is isotopically (^{3}He/^{4}He and δ^{13}C–CO_2) identical to fumaroles, showed a very low δ^{15}N value of −2.6‰, which is not consistent with positive values for fumaroles (+2.2‰ to +3.5‰). The explanation for this low δ^{15}N is unclear, however it might be an artifact produced during analysis, due to the low voltage of this sample in comparison to the other samples and air standards (5 times less N in sample MKW-2).

Tarumae samples, in particular the fumaroles, had chemical and isotopic gas compositions that are more complex than those described for Tokachi and Meakan volcanoes.

As shown in Fig. 3, Tarumae volcano had high $CO_2/^3$He ratios for fumarole samples (up to 5.36×10^{11}), closer to the crater, and comparatively low $CO_2/^3$He ratios for hot spring samples (up to 1.06×10^{10}), further away from the crater. This negative trend is consistent with the low fumarole (~3.09Ra) and the high hot spring (~5.72Ra) Rc/Ra. However, these results are in disagreement with data reported by Sano et al. (1998a), where ^{3}He/^{4}He ratios decreased and $CO_2/^3$He ratios increased with distance from the crater. Furthermore, Sano and Wakita (1988) reported Rc/Ra and ^{4}He/^{20}Ne ratios from Tarumae hot springs of 3.12Ra and 1.4, respectively. Although we found similar ^{4}He/^{20}Ne ratios as those reported by Sano and Wakita (1985), our Rc/Ra values were 1.5 to 2 times higher. An explanation for these results is given in the following section.

Fig. 4 presents the ^{3}He–^{4}He–CO_2 ternary plot. Fumarole and bubbling gas samples from Meakan and Tokachi are plotted together with Tarumae hot spring samples for comparison. As pointed out by Giggenbach et al. (1993), this diagram can be used to identify binary mixing of volatiles and loss and/or addition of specific volatile phases (e.g. CO_2, He) by linear trajectories on the plot. Based on Fig. 4, our samples can be divided into two different groups:

1) Tarumae hot spring samples (TAW-4, TAW-5), plus Meakan (MK-4, MKW-2) and Tokachi (TOK4, TOK-6) samples. All plot in or next to the volcanic arc field, with a high Rc/Ra ratio (7.36Ra to 5.87Ra) and a low $CO_2/^3$He ratio. This is consistent with the admitted subduction zone value ($1.5 \pm 1.1 \times 10^{10}$; Sano and Williams, 1996).
2) Tarumae fumarole samples (TA-1 and TA-2) plot close to the CO_2 apex and have exceptionally high $CO_2/^3$He ratios and relatively low Rc/Ra values. We argue that the very low ^{3}He/^{4}He, and by consequence the high $CO_2/^3$He values of Tarumae fumaroles correspond to CO_2 and a radiogenic ^{4}He addition in the hydrothermal system.

Additionally, our high fumarole $CO_2/^3$He results are apparently not consistent with the low fumarole δ^{13}C–CO_2 values (−6.34‰ and

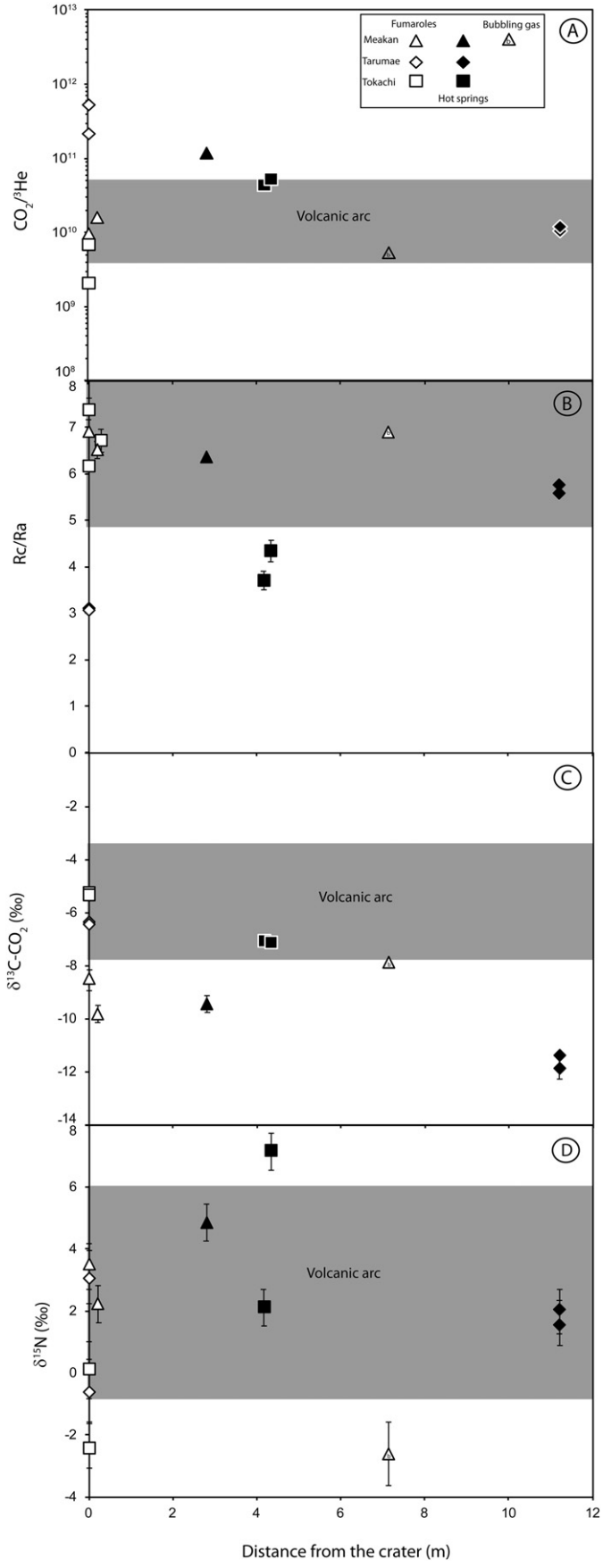

Fig. 3. $CO_2/^3He$ (A), Rc/Ra (B), $\delta^{13}C$–CO_2 (C) and $\delta^{15}N$ (D) versus the distance from the volcanic vent for Tarumae, Tokachi and Meakan volcanoes. Decreasing of Rc/Ra and $\delta^{13}C$–CO_2 and simultaneous increasing of $CO_2/^3He$ and $\delta^{15}N$ as a function of the distance from the volcanic vent, indicates crustal contamination by local sediments. The error is equivalent to the size of the symbols when not observable.

−6.43‰), which are similar to the value for volcanic arcs, −5.5 ± 2.2‰ (Sano and Marty, 1995) and −7.5‰ to −2.1‰ (Hernandez et al., 2001a). Our hot spring samples had low $\delta^{13}C$–CO_2 values, −11.86‰ (TAW-4) and −11.37‰ (TAW-5; Fig. 3c), but normal $CO_2/^3He$ ratios (1.06×10^{10}). These results can be explained by a combination of crustal fluid contamination from organic sediments (−40‰ to −20‰; Hoefs, 2009) during transport of the magmatic fluids, and CO_2 loss by a calcite precipitation at 25 °C (Hilton et al., 1998). At a temperature of 25 °C, calcite is enriched in ^{13}C relative to residual CO_2, thus the fractionation factor is −10‰ that produces a decrease of $CO_2/^3He$ and $\delta^{13}C$–CO_2 values (Ray et al., 2009). Based on our results, we infer that two distinct processes affected the Tarumae hot springs and the Tarumae fumaroles. Tarumae hot springs were partially affected by crustal fluid contamination related to water-rock interaction and CO_2 loss by calcite precipitation, which affected more strongly $\delta^{13}C$–CO_2 values than Rc/Ra ratios. However, Tarumae fumaroles seem to be affected by strong crustal contribution at shallow level and/or at the surface of the dome (see next section). Thus, Rc/Ra from Tarumae hot springs appear more representative of the magmatic source than Rc/Ra from Tarumae fumaroles.

5.3. Tarumae fumaroles and their relationship with dome evolution

5.3.1. Degassed magma from the dome

A lava dome is formed after a non-explosive extrusion, and grows by a combination of intrusive and extrusive addition of magma, either as single continuous events or through a series of small pulses, which together build a larger dome. However, if solidification and strengthening of the dome's interior occurs more rapidly than the generation of buoyancy in the magma chamber, it becomes difficult for new magma to reach the surface, and the eruption shuts down. Furthermore, the deep-seated processes to release the continuously generated magma over pressure become progressively less efficient and magma production decreases (Anderson and Fink, 1989; Fink et al., 1990). At Galeras volcano, solidification and strengthening of the crust of the dome was sufficient to isolate the lower part of the magma column which behaved more as a closed system, with volatile production. Thus, the less vesiculated material was located at the surface and at very shallow levels, while the highly vesiculated magma remained at deeper levels where most degassing takes place (Calvache and Williams, 1997).

Mount St. Helens volcano is a good example of a lava dome that has presented persistent fumarole activity since 1980. Casadevall et al. (1983) studied the gas emissions of Mount St. Helens between 1980 and 1982. Eight months after the eruption of May 1980, which was characterized by a large emission rate of SO_2 (1300 t/d) and CO_2 (10,000 t/d), the eruption activity turned extrusive, with production of viscous lava that eventually formed a dome. During this period of non-explosive extrusion, the emission rate of SO_2 and CO_2 decreased to 140 t/d and 1100 t/d, respectively. The long-term decrease in overall production suggests that magma degassing in the upper part of the dome was complete.

Tarumae volcano has had an andesitic lava dome in its center since 1909. Since the last eruption in 1981, the dome with two big fractures persistently degasses through strong fumarole activity in the summit area. The current overall shape of the dome was established in 1933. Our chemical results of Tarumae fumaroles show low SO_2/H_2S and high CO_2/S ratios (from 0.5 to 0.8 and 5 to 11, respectively) in comparison to Tokachi fumaroles (3.3 and 1.6, respectively) (Table 2). Furthermore, the CO_2/SO_2 ratio of Tarumae fumaroles increased from 2003 (0.89–1.46; (Shinohara, 2005) to 2012 (17.9–24.5). This argues for the decrease of SO_2 associated with a low amount of H_2S and HCl,

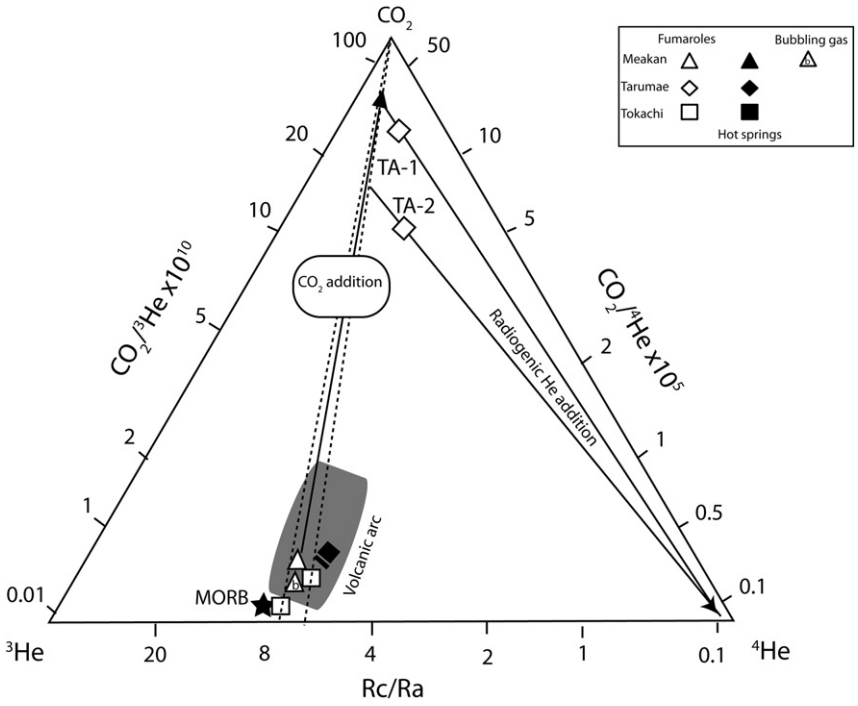

Fig. 4. Ternary diagram between ^{3}He, ^{4}He and CO_2 for fumarolic and bubbling gases from Tarumae, Tokachi and Meakan, and hot springs from Tarumae, adapted from Giggenbach and Poreda (1993). Hot springs from Tokachi and Meakan are not reported because they are affected by crustal contamination and do not represent the magmatic source. For comparison, MORB (black star) and volcanic arc (gray domain) fields are reported (Marty et al., 1989; Sano and Marty, 1995; Sano and Williams, 1996; Fourre et al., 2002; Hilton et al., 2002). The high $CO_2/^3$He and low Rc/Ra for Tarumae fumaroles, in comparison with other fumaroles, is the result of CO_2 and radiogenic ^{4}He addition. Symbols: diamond for Tarumae, square for Tokachi and triangle for Meakan.

suggesting that the lava dome presented significant magma degassing of its volatiles, as an open system. Thus, the degassed lava dome is the result of the absence of a new magmatic pulse. This proposition is supported by Mori et al. (2006), who showed that low volatile emissions observed at Tarumae in 2003–2004 reflected the lack of open-vent degassing (and strong interaction with the hydrothermal system).

5.3.2. Radiogenic ^{4}He addition from superficial aquifer in degassed magma

Considering that the Tarumae dome is internally highly fractured and altered by fumarolic activities (Hernandez et al., 2001a; Yamaya et al., 2009), penetration of meteoric water through the factures to the inside of the dome is likely. Furthermore, tomographic resistivity studies show the existence of an aquifer located between 50 m and 150 m under the dome (Yamaya et al., 2009). Mori et al. (2006) argued that low volatile emission observed at Tarumae in 2003–2004 was part of the strong interaction with the hydrothermal system. Therefore, it is possible that water-rock interaction is responsible for the release of radiogenic ^{4}He that would have reduced the magmatic ^{3}He/^{4}He ratio of the fumaroles. Finizola et al. (2002) provided evidence for a hydrothermal system under the summit of Stromboli volcano. Others found similar differences of the He isotopic ratios between fumaroles (3.1Ra) and hot springs (4.1Ra) as for Tarumae volcano (Inguaggiato and Rizzo, 2004). Therefore, it is highly likely that the low ^{3}He/^{4}He ratios observed in Tarumae fumaroles are the result of a large contribution of radiogenic ^{4}He due to the presence of a shallow aquifer and the penetration of meteoric water through fractures. The high amounts of CH_4 and N_2 measured in Tarumae fumaroles argue also for contamination by crustal materials. It is important to note that radiogenic ^{4}He contribution from the crust can occur in the hydrothermal system which is located under the dome but also in a deeper hydrothermal system.

Considering that the composition of Tarumae fumaroles is close to the CO_2 apex in Fig. 4, high $CO_2/^3$He ratios could be the result of CO_2 addition from the crust. This suggests that δ^{13}C–CO_2 values for Tarumae fumaroles (−6.34‰ and −6.43‰) are the lower limit of carbon composition for the Tarumae magmatic source.

5.4. Explanation for different ^{3}He/^{4}He ratios between hot springs and fumaroles at Tarumae

As observed for Mount St. Helens between 1980 and 1982, solidification and strengthening of the crust of the dome could be sufficient to isolate the deep lower part of the magma column (as a closed system) that allows volatile production. At the same time, the upper part of the dome degasses most of its volatiles. In this case, it is acceptable to conclude that the lower part of the magma column keeps the initial magmatic signature, such as a high ^{3}He/^{4}He ratio.

Fig. 5 shows a schematic model of fluid circulation under the Tarumae volcanic area and the relationship between fumaroles and hot springs. The model from Fig. 5A is supported by the tomographic resistivity results of Yamaya et al. (2009). Tarumae dome is isolated from the deep part of the magmatic conduit by solidification and strengthening of its crust. Thus, the large degassed magma from the dome reduces the emission rate of magmatic volatiles such as SO_2 and CO_2 in fumaroles. The addition of radiogenic ^{4}He in the shallow system induces a decrease in ^{3}He/^{4}He ratios. The deeper part of the magma conduit is isolated from the surface and may keep the initial magmatic signature (≈6Ra), still allowing closed-system volatile release through fluid circulation. In this way, the hydrothermal system of the volcano remains active. Because fluids cannot escape through the dome, an alternative path is needed. This path must lie in a zone affected by fractures, permeable layers, and/or areas of hydrothermal manifestations. Hot spring zones are perfect candidates. Tarumae hot springs that in 1982 presented ^{3}He/^{4}He ratio of 3.72Ra (Sano and Wakita, 1985) now have a higher ^{3}He/^{4}He ratio of 5.72Ra, more similar to a magmatic He signature, but also affected by crustal ^{4}He addition from host rocks and water from Shikotsu lake.

Another alternative to explain the high ^{3}He/^{4}He of Tarumae hot springs may be that the source is not Tarumae volcano itself, but a magma chamber beneath the Shikotsu caldera (Shikostu lake, Fig. 5B). This alternative model was accepted in the case of Aira Caldera (Kyushu, Japan), composed by Sakurajima volcano and Wakamiko submarine crater. Sakurajima volcano is an active volcano, whereas Wakamiko

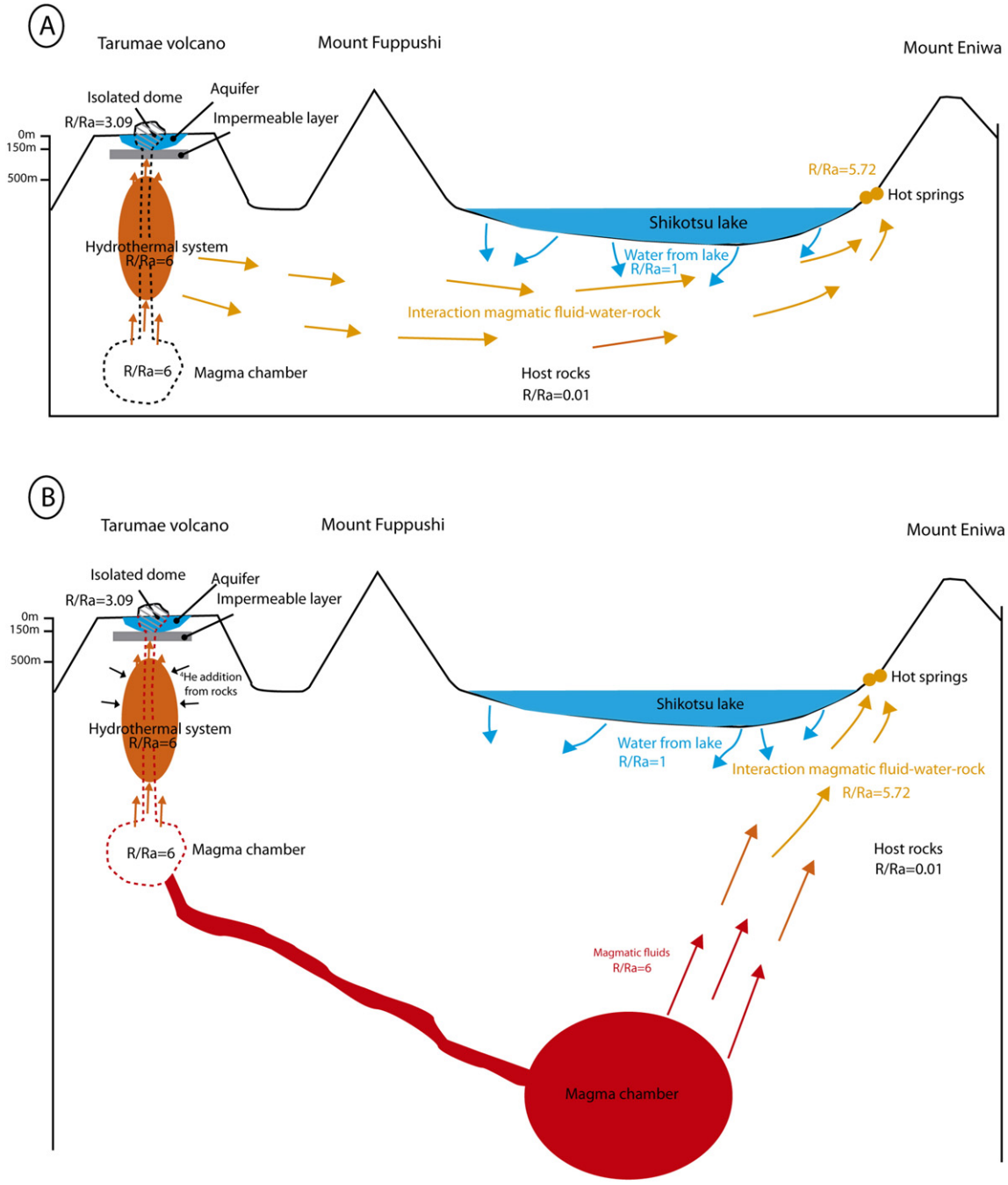

Fig. 5. A) Schematic model of fluid circulations in Tarumae area and Shikotsu Caldera. Model based on tomographic resistivity study from Yamaya et al. (2009). B) Schematic model that implies a magmatic chamber under Shikotsu Lake to explain high $^{3}He/^{4}He$ ratios in hot springs from Tarumae. R/Ra for water and host rocks are from Sano and Wakita (1988), and hot springs, fumaroles and magmatic chambers are from our study.

crater is characterized by strong fumarolic emanation from the seafloor. Sakurajima and Wakamiko crater showed a similar $^{3}He/^{4}He$ mantle source around 7.2 ± 0.8Ra (Roulleau et al., 2013). However, Sakurajima CO_2 (1800 t/d) and ^{3}He (0.71 mol/y) fluxes appear higher than those of Wakamiko (CO_2: 184 t/d and ^{3}He: 0.001 mol/y), indicating that degassing is higher at Sakurajima. Thus, fluid emission from Wakamiko crater which is commonly explained as a manifestation of the Aira caldera activity, does not demonstrate that fluids are transported from Sakurajima volcano (Aramaki, 1984; JMA, 2012; Roulleau et al., 2013).

Thus, this alternative model suggests a limited connection between Tarumae fumaroles (or Tarumae volcano) and Tarumae hot springs. In this case, it is possible that addition of radiogenic ^{4}He occurs in the shallow hydrothermal system (hydrothermal–crustal interaction) of Tarumae volcano. This in turn produces the decrease of $^{3}He/^{4}He$ ratios observed in Tarumae fumaroles (Fig. 5B).

5.5. Helium in phenocrysts of Tarumae pumices

The helium isotopic ratio in olivine and pyroxene phenocrysts is used to investigate and characterize magma/mantle compositions and physical processes. Helium isotopic compositions from fumaroles and minerals provide evidence for degassing processes in Tarumae fumarole samples. We analyzed olivine and pyroxene in a Tarumae pumice sample from the 1739 eruption. The olivine $^{3}He/^{4}He$ ratio was higher

(5.22Ra) than for cogenetic pyroxene (3.73Ra). It is recorded that the variation of $^3He/^4He$ signatures in cogenetic olivine and pyroxene is the result of multiple processes such as the preferential He diffusion (preferential ^3He loss) in pyroxene at magma temperature and addition of radiogenic ^4He by crustal contamination in the magmatic chamber (Trull and Kurz, 1993; van Soest et al., 2002).

The relatively large difference in mass between ^3He and ^4He can also produce a large difference in diffusion (Trull and Kurz, 1993; Shaw et al., 2006). Harrison et al. (2004) calculated that the $^3He/^4He$ ratio in phenocrysts from Siberian lavas can decrease drastically from 8Ra to 4Ra in several years (~60 years) when the fraction of He lost is 0.98. Thus, the authors found a correlation between decreasing $^3He/^4He$ and decreasing He content, suggesting that He can potentially diffuse from the phenocryst to the magma depending on temperature (Trull and Kurz, 1993). Furthermore, it is known that there is a preferential diffusion exchange of magmatic He in pyroxene in comparison with olivine, with a He diffusion estimated to be 10 times higher in pyroxene than in olivine (Trull and Kurz, 1993). For example, in the pumice samples from Tarumae, we expected a lower He content in pyroxene than olivine. However, this was not the case; pyroxene had a He content of 1.5×10^{-9} cm^3STP/g while in olivine it was 9.7×10^{-10} cm^3STP/g. Thus, the preferential diffusion process does not explain the $^3He/^4He$ variation in olivine and pyroxene.

The second possibility is to estimate a radiogenic ^4He addition from the crust into the magmatic plumbing system. As magma ascends to the surface, it experiences rapid cooling at its margins, where it comes in contact with the surrounding crust (Danyushevsky et al., 2004). This rapid cooling facilitates crystallization and newly formed phenocrysts in close proximity to the surrounding host rocks, a source of radiogenic ^4He. Furthermore, crystallization and the system closure in mineral species are strongly dependent on temperature. This concept of closure temperature for mineral species were discussed for the first time by Dodson (1973) to relate cooling rates to diffusion parameters for different species. The mobility of species (by diffusion) is controlled by temperature (Hilton et al., 1995; van Soest et al., 2002), and the He closure temperature is higher for olivine than for pyroxene. Hence olivine will tend to better preserve the primary composition of the magma, whereas pyroxene's lower closure temperature will allow He diffusion and exchange with the magma (and/or surrounding host rocks). As observed by Trull and Kurz (1993), He in pyroxene diffuses ten times more quickly than in olivine, supporting this hypothesis. Thus, the addition of radiogenic ^4He in pyroxene related to the diffusion of He from the crust, produces the decrease of the $^3He/^4He$ ratio and the increase in He content. If we consider that the He content for Tarumae is higher in pyroxene than in olivine, and that the $^3He/^4He$ ratio is higher in olivine than pyroxene (Table 3), we conclude that the most viable interpretation of our data is the diffusion of radiogenic ^4He in pyroxene from the surrounding crust (Hilton et al., 1995; van Soest et al., 2002).

Olivine is considered to represent the most primitive composition of the magma. Thus, the $^3He/^4He$ ratio observed for Tarumae (5.22Ra) must represent the initial $^3He/^4He$ of the Tarumae magma. The ratio of $^3He/^4He$ observed in Tarumae olivines is close to the observed $^3He/^4He$ ratio for hot springs (5.24Ra and 4.68Ra), and consistent with a magmatic source for Tarumae around 6Ra (Fig. 2). This result supports the hypothesis that the Tarumae fumarole samples are modified by the addition of radiogenic ^4He, producing the lower $^3He/^4He$ ratio in comparison to the $^3He/^4He$ ratios observed in hot spring samples.

5.6. Isotope signature of the magma source

5.6.1. Helium magmatic source

Helium isotope compositions in subduction zones range between 5Ra to 8Ra (Marty et al., 1989; Poreda and Craig, 1989; Sano and Marty, 1995; Sano and Williams, 1996; Fourre et al., 2002). Based on the correlation between $^3He/^4He$ versus $^4He/^{20}Ne$ (Fig. 2a–c), we can approximate the He magmatic source for each volcano, i.e., 6Ra for Tarumae, 7Ra for Meakan, and 7.5Ra for Tokachi. Tarumae He isotope composition was only calculated using the hot spring samples, and hence represented the lowest limit for this volcano. The Usu volcano is located ~50 km from the Tarumae volcano and has a Rc/Ra ranging between 6.63Ra and 7.05Ra (Nagao et al., 1981; Giggenbach and Matsuo, 1991; Hernandez et al., 2001b). These He isotopic ratios suggest that Tarumae $^3He/^4He$ composition is slightly higher than Tarumae hot springs. However, these results are within the accepted subduction zone range, showing that the small He isotopic variations observed in Hokkaido volcanoes respond to variation of the deep source composition, being associated to heterogeneous mantle wedge related to the increasing of the decarbonation of subducted slab (Snyder et al., 2001).

5.6.2. Nitrogen and argon magmatic source

As shown above, N and Ar modified by air contamination related to meteoric circulation in the hydrothermal system, and during sampling. This is a typical feature of arc volcanoes, with $N_2/^{40}Ar$ and $^{40}Ar/^{36}Ar$ usually lower than 1000 and 400, respectively (Sano et al., 2001; Hilton et al., 2002).

Fig. 6 shows $N_2/^{36}Ar$ and $^{40}Ar/^{36}Ar$ ratios for Tarumae (TA-1, TA-2), Tokachi (TOK-4, TOK-6), and Meakan (MK-4) fumarole samples, as well as for the crust, MORB, and volcanic arc field (Marty and Zimmermann, 1999; Sano et al., 2001). Our Hokkaido fumarole samples define a positive trend that fits well with the accepted volcanic arc field and plots toward the crust end-member, far from the mantle-ASW mixing line defined by Fischer et al. (2009). This evidence supports a model for involvement of a crustal component to explain the nitrogen and argon compositions of Hokkaido volcanoes (Sano et al., 2001). This positive correlation also highlights the variation of nitrogen and argon compositions at the three volcanoes as a result of deep source variation. This could be the consequence of either fluctuating subducted sediment compositions, or varying amounts of subducted sediments incorporated into the mantle wedge as proposed in previous studies (Sano et al., 1998b; Hilton et al., 2002). As shown in the previous section, Tarumae fumaroles are affected by hydrothermal-crustal interaction. Thus, it is important to take into account that Tarumae fumarole $N_2/^{36}Ar$ and $^{40}Ar/^{36}Ar$ ratios are most likely increased by this process.

To better constrain the signature of the deep source, and determine the proportions of all components involved, we present a plot of $\delta^{15}N$ versus $N_2/^{36}Ar$ (Fig. 7) where the nitrogen compositions for Tarumae, Tokachi, and Meakan volcanoes define a mixing line between three components (Sano et al., 2001; Marty and Dauphas, 2003): ASW (0‰; 1.1×10^4), crust ($+7 \pm 4$‰; 6×10^6), and mantle (-5‰; 6×10^6). The mixing curve is as follows:

$$\delta^{15}N_{obs} = A\ \delta^{15}N_{ASW} + M\ \delta^{15}N_{Mantle} + S\ \delta^{15}N_{Sed} \quad (7)$$

$$1/\left(N_2/^{36}Ar\right)_{obs} = A/\left(N_2/^{36}Ar_{ASW}\right) + M/\left(N_2/^{36}Ar_{Mantle}\right) + S/\left(N_2/^{36}Ar_{Sed}\right) \quad (8)$$

$$Mantle + Sed + ASW = 1 \quad (9)$$

where *obs*, *ASW*, *Mantle*, and *Sed* refer to: the observed value, ASW, mantle, and sediments, respectively. Calculations are presented in Table 4.

Meakan fumaroles have a low $N_2/^{36}Ar$ (up to 3.7×10^4), but slightly higher than the air component, and a higher $\delta^{15}N$ that ranges from $+2.2 \pm 0.7$‰ to $+3.5 \pm 0.7$‰. We found that the nitrogen fumarole signature of Meakan is composed of 50.7% sediments, 49% air, and 0.3% mantle. Tokachi fumaroles have $\delta^{15}N$ values ranging between -2.4 ± 0.7‰ and $+0.1 \pm 0.9$‰, and the lowest $N_2/^{36}Ar$ ratio (as low as 2.3×10^4), close to the air value. The nitrogen signature of these fumaroles is dominated by air (67%–72%) and mantle (33.8%–14.5%), with minor contribution from sediments (0.2%–13.5%). Tarumae

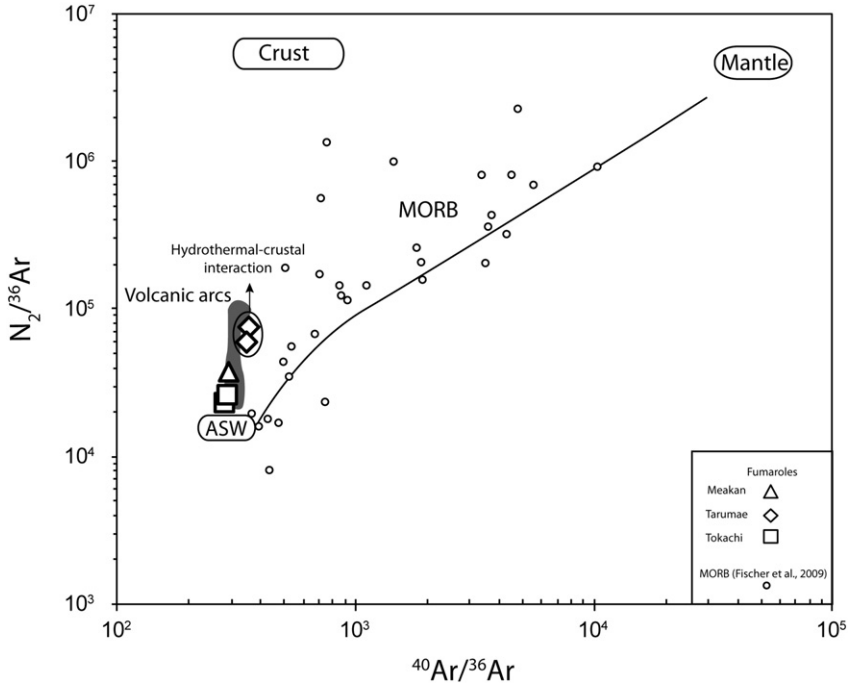

Fig. 6. $N_2/^{36}Ar$ and $^{40}Ar/^{36}Ar$ ratios for Tarumae, Tokachi, and Meakan fumarole samples, as well as for the crust, MORB, and arc volcanoes fields (Marty and Zimmermann, 1999; Sano et al., 2001). The positive correlation of our samples shows the mixing between three components, ASW, MORB and crust from subducted sediment. The mantle-ASW mixing line is defined by Fischer et al. (2009) based on MORB data. A possible hydrothermal–crustal interaction affects Tarumae fumaroles, which increases $N_2/^{36}Ar$ and $^{40}Ar/^{36}Ar$ ratios.

fumaroles have intermediate compositions with $\delta^{15}N$ values ranging from -0.6 ± 1.1‰ to $+3.1 \pm 0.7$‰. The average Tarumae hot spring $\delta^{15}N$ value was $+1.9$‰ (not reported in Fig. 7), consistent with the range of Tarumae fumaroles. The highest $N_2/^{36}Ar$ (up to 7.5×10^4) observed for Tarumae fumaroles and high N_2 content in TA-2 suggest crustal N_2 addition. This means that the real nitrogen signature of Tarumae is defined between TA-2 and TA-1 compositions; which are composed of 16%–39.5% mantle, 61%–30.5% sediments, and 23%–30% air (Table 4). Large variations in mantle, sediment and air contribution for Tarumae fluids are the result of hydrothermal–crustal interaction and show the limitation of the model. The average $\delta^{15}N$ value of Tarumae hot springs ($+1.9$‰) is probably a good candidate for the nitrogen signature of Tarumae.

Based on these nitrogen isotope data, we demonstrate that the contribution from subducted sediments is higher at Meakan and Tarumae volcanoes compared to Tokachi volcano, which is consistent with the

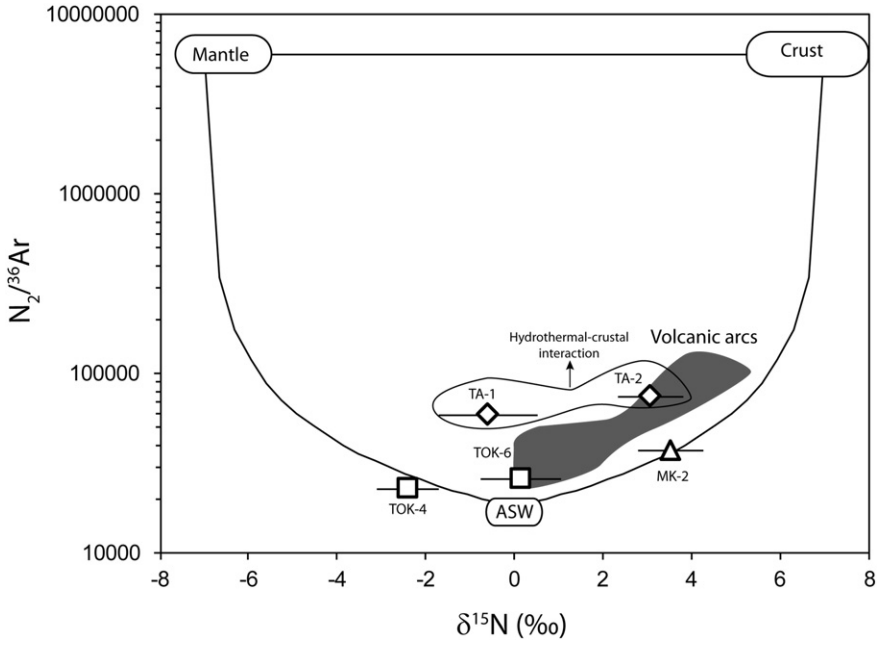

Fig. 7. $\delta^{15}N$ versus $N_2/^{36}Ar$ for Tarumae (diamond), Tokachi (square) and Meakan (triangle) fumarole samples. Our samples are explained by a mixing between three components (Sano et al., 2001; Marty and Dauphas, 2003): ASW (0‰; 1.1×10^4), crust ($+7 \pm 4$‰; 6×10^6), and mantle (-5‰; 6×10^6) that are illustrated by solid lines. Volcanic arc data (gray field) are from Sano et al., 2001. Bubbling gas sample from Meakan is not reported because its $\delta^{15}N$ value appears to represent an artifact during analysis. A possible hydrothermal–crustal interaction affects Tarumae fumaroles, which increases $N_2/^{36}Ar$ ratios.

Table 4
Nitrogen and carbon contribution models for fumarole and bubbling gas samples.

	Nitrogen contribution			Carbon contribution			L/S	(L + S)/M
	Air %	Mantle %	Sediment %	Limestone %	Mantle %	Organic sed. %		
TA-2	23	16	61	67[a]	15[a]	18[a]	3.7[a]	5.7[a]
TA-1	30	39.5	30.5	67[a]	15[a]	18[a]	3.7[a]	5.7[a]
TOK-4	67	33.75	0.25	63	25	12	5.3	3.0
TOK-6	72	14.5	13.5	37	58	5	7.4	0.7
MK-4	49	0.3	50.7	58	18	24	2.4	4.6
MKW-2	–	–	–	50	30	20	2.5	2.3

Note:
[a] Tarumae carbon contributions are calculated using the $CO_2/^3He$ ratio equal to 10×10^9, similar to Tarumae hot springs.

higher $^3He/^4He$ ratios of Tokachi samples. Mantle contribution is higher of two orders of magnitude in Tokachi than Meakan fluids.

5.6.3. Carbon magmatic source

One approach to assess the carbon origin in subduction zones is the three-component mixing model proposed by Sano and Marty (1995). Based on their $CO_2/^3He$ and $\delta^{13}C$–CO_2 characteristics, samples are described by a carbon mixture made of marine carbonates, mantle and organic sediments. $\delta^{13}C$–CO_2 of the MORB component is $-6.5 \pm 2.5‰$ (Sano and Marty, 1995; Sano and Williams, 1996). In contrast, $\delta^{13}C$–CO_2 of sediments varies between two major components (Hoefs, 2009): organic sediments ($-40‰$ to $-20‰$) and marine sediments ($0 \pm 2‰$). Fumarolic gases in subduction zones have $\delta^{13}C$–CO_2 of $-5.5 \pm 2.2‰$ (Sano and Marty, 1995; Sano and Williams, 1996; Snyder et al., 2001). The mixing curve follows:

$$\delta^{13}C{-}CO_{2obs} = L\ \delta^{13}C_{Lim} + M\ \delta^{13}C_{Mantle} + S\ \delta^{13}C_{Sed} \quad (10)$$

$$1/\left(CO_2/^3He\right)_{obs} = L/\left(CO_2/^3He_{Lim}\right) + M/\left(CO_2/^3He_{Mantle}\right) + S/\left(CO_2/^3He_{Sed}\right) \quad (11)$$

$$Lim + Mantle + Sed = 1 \quad (12)$$

where *obs*, *Lim*, *Mantle*, and *Sed* refer to: the observed value, limestone, mantle and sediments, respectively. Results of the calculations are presented in Table 4.

Our data from Hokkaido volcanoes are plotted in Fig. 8 along with data from Kirishima and Satsuma-Iwojima, Kyushu, for comparison (Sato et al., 1999, 2002). As argued above, Tarumae fumaroles are affected by hydrothermal–crustal interaction inducing an increase in the $CO_2/^3He$ ratio without modification of the magmatic $\delta^{13}C$–CO_2. The magmatic source of Tarumae can be characterized by a mean fumarole $\delta^{13}C$–CO_2 of $-6.39 \pm 0.06‰$. However, the true magmatic $CO_2/^3He$ signature is difficult to define. We assume here that $CO_2/^3He$ of Tarumae fumaroles is at least 1×10^{10}, which represents the lower $CO_2/^3He$ of hot springs and in the range of typical volcanic arc (Sano and Williams, 1996). Based on this assumption, the estimated proportions of the different components involved are: 67% limestone, 18% organic sediments, and 15% mantle (Table 4). Considering that the Tarumae basement is constituted only by Miocene/Pliocene subaqueous volcanic and sedimentary rocks (Doi, 1957), the high carbon contribution from limestone mostly derived from the subducted slab.

Tokachi fumaroles have a $CO_2/^3He$ ranging from 2.12×10^9 to 6.99×10^9, and a mean $\delta^{13}C$–CO_2 of $-5.28 \pm 0.06‰$. These values are very similar to the mantle field (2×10^9 and $-6.5 \pm 2.5‰$, respectively). The estimated proportions that explain the Tokachi fumaroles range between 25% and 58% of the mantle component, and 37%–63% of the

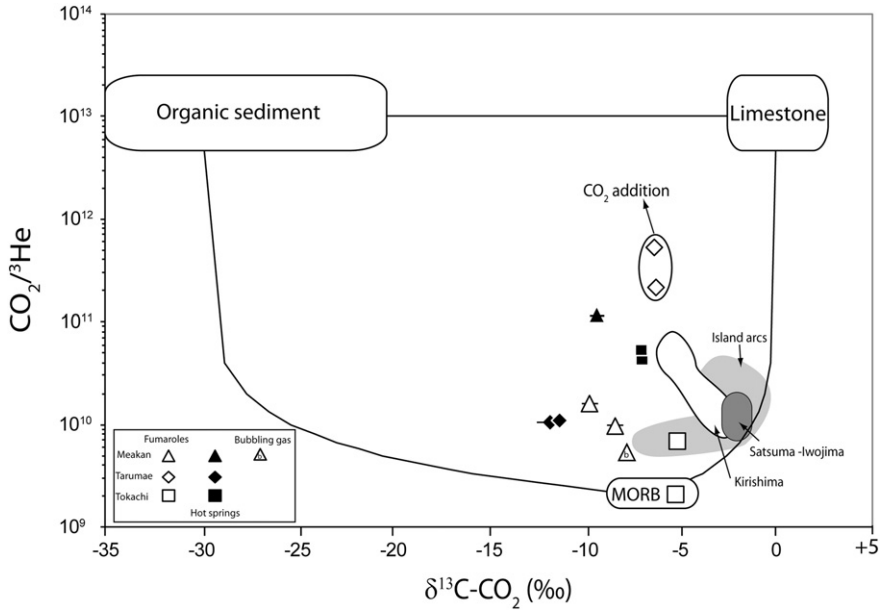

Fig. 8. $CO_2/^3He$ versus $\delta^{13}C$–CO_2 for Tarumae, Tokachi and Meakan samples compared to MORB, organic sediments and marine limestone. The solid lines represent mantle-organic sediments, mantle-marine limestone, and organic sediments-marine limestone binary mixing lines. MORB has $\delta^{13}C$–$CO_2 = -6.5 \pm 2.2‰$ and $CO_2/^3He = 2 \times 10^9$ (Marty et al., 1989; Sano and Marty, 1995; Sano and Williams, 1996). $\delta^{13}C$–CO_2 and $CO_2/^3He$ value for organic sediments are $-30 \pm 10‰$ and 1×10^{13} (Sano and Marty, 1995; Hoefs, 2009) and are $0 \pm 2‰$ and 1×10^{13} for marine limestone (Sano and Marty, 1995; Hoefs, 2009), respectively. Island arc field represents fumarole data from Sano and Marty (1995). Satsuma-Iwojima and Kirishima data are from Sato et al. (1999; 2002).

limestone component, suggesting that carbon comes mainly from the mantle and slab (c.f. limestone; Table 4).

Meakan fumarole (MK-4) and bubbling gas (MKW-2) samples had an average $\delta^{13}C$–CO_2 of -8.16 ± 0.43‰ and a $CO_2/^3He$ of 5.43×10^9 to 9.80×10^9. These values clearly suggest that the organic sediment contribution in the Meakan magmatic source is higher than for Tokachi and Tarumae. Our calculations yielded the following estimates: 20–24% organic sediments (only 12% for Tokachi), 50%–58% limestone, and 18%–30% mantle (Table 4).

Importantly, the carbon composition variations observed in Tarumae, Tokachi, and Meakan volcanoes are not restricted to this isotope system, and are also observed in He, N, and Ar isotopes. This leads to the conclusion that the magmatic source for these three volcanoes depends mainly on the variation of the contribution of subducted sediments vs. mantle wedge.

5.7. Geographic variations of isotopic composition in Hokkaido versus distance from volcanic front

Isotopic and geochemical variations along volcanic arcs have been observed in subduction zones, such as in Central America (Shaw et al., 2003; Elkins et al., 2006) and Indonesia (Sangihe and Sunda Arc; Clor et al., 2005; Halldorsson et al., 2013; Hilton et al., 1992; Hilton and Craig, 1989; Jaffe et al., 2004). In the case of Hokkaido, the direction of the Pacific Plate subduction changes from N–S along the Honshu Trench, (southwestern Hokkaido) to WSW–ESE along the Kurile Trench (northeastern Hokkaido). Such modification of the subducted plate direction can affect magmatism in Hokkaido. It may be recognized and constrained by looking at the distribution of the volcanic centers with respect to the volcanic front versus their isotopic compositions.

We noted variations in the isotopic compositions of Hokkaido volcanoes. Fig. 9 shows the He, C, and N isotopic ratios vs. longitude and plotted data from Usu volcano support Tarumae data (Nagao et al., 1981; Giggenbach and Matsuo, 1991; Hernández et al., 2001). The gray field represents the range of magmatic source composition for each volcano. One of the particularities is that Tokachi fumaroles have higher Rc/Ra, higher $\delta^{13}C$–CO_2, and lower $\delta^{15}N$ compared to Tarumae and Meakan fumarole and bubbling gases. These variations can reflect several processes: (1) variability in the composition of subducted sediment chemistry; (2) increase in the volume of subducted sediments under the arc, or (3) change in the thermal regime experienced by the subducting slab related to the onset of collision.

(1) *Variability in the composition of subducted sediment chemistry*. An important parameter used to compare output fluxes in different arcs is the L/S ratio (i.e. fraction of C derived from a limestone source (L) that derived from an organic sediment (S) component). The worldwide average arc L/S value (Hilton et al., 2002) is 6.0 ± 3.8 (assuming $S = -30$‰; Hoefs, 2009); and the average values for Tokachi and Meakan are 6.3 ± 1.5 and 2.3 ± 0.3, respectively (Table 4). The L/S value for Tarumae is estimated at ~3.7 (Table 4), not very different from the Meakan value. Such a high value for Tokachi could reflect a carbonate-rich source, compared to Meakan and Tarumae. Deep sea drill sites (ODP 1179 and DSDP 193) in the Kurile arc show no lateral variation in sediment lithology, which are composed of 250 m of diatom-bearing radiolarian ooze, 40 m of pelagic clay, and 100 m of chert (Dreyer et al., 2010). Sediments of the Honshu trench are mainly composed of organic sediments, such as clays and silt (von Huene and Arthur, 1982). Altogether, there is no large difference in the subducted sediment lithology between Tokachi, Meakan, and Tarumae. This suggests that the preferential incorporation of limestone or slab component is not a valid option to explain the high $\delta^{13}C$–CO_2 ratio from Tokachi volcano.

(2) *Increase in the volume of subducted sediments under the arc*. Another hypothesis is to use the ratio (L + S)/M as a marker for difference in the relative slab contribution (L + S) versus mantle contribution (M). Our results for these calculations are presented in Table 4. Tokachi average ratio is 1.9, whereas it is 5.3 for Tarumae and 3.4 for Meakan, suggesting an enhanced slab C contribution for Tarumae and Meakan fumaroles, and a higher mantle contribution for Tokachi fumaroles. Nitrogen contribution (Table 4) also shows that the sediment contribution for Tokachi volcano is lower (0.25%–13.5%) than for Tarumae (30.5%–61%) and Meakan (50.7%). This is consistent with the highest $^3He/^4He$ Rc/Ra (7.5Ra; Fig. 9) observed in Tokachi. Additionally, both Meakan and Tarumae have low $^3He/^4He$ Rc/Ra consistent with a higher contribution from the slab. These isotopic characteristics for Tarumae and Meakan are also consistent with the fact that Kurile and Honshu arcs are presently non-accretionary (erosive margin), so that most sediments are subducted (Kita et al., 1993; Dreyer

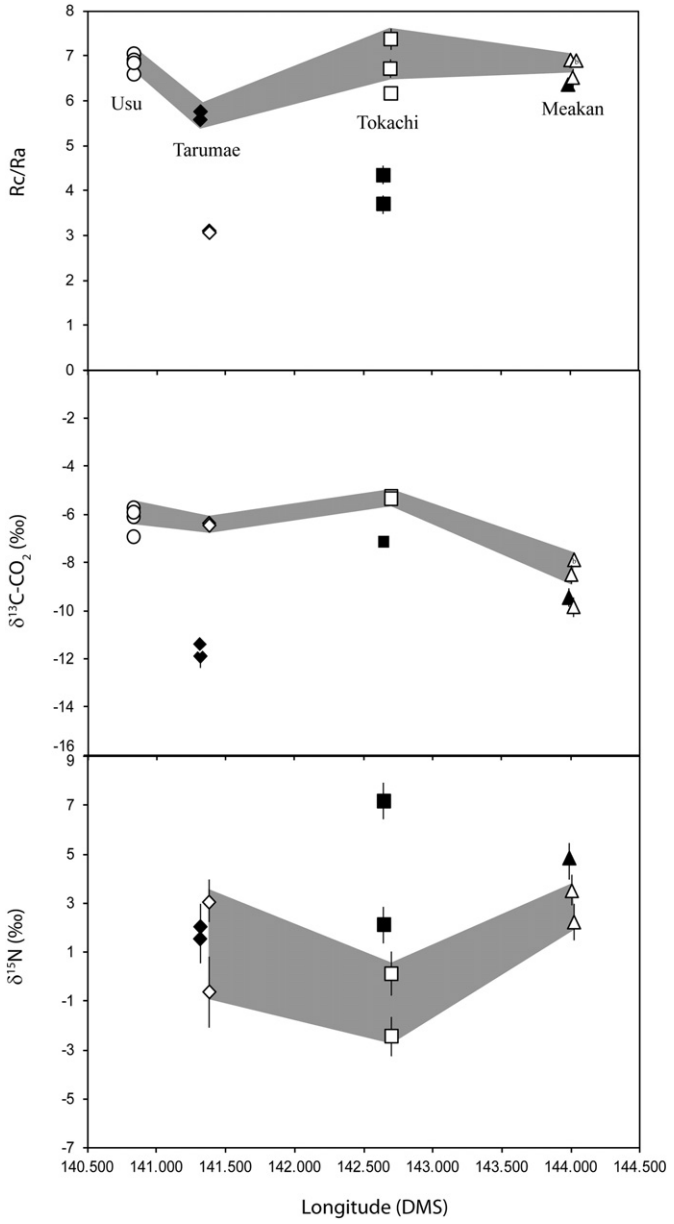

Fig. 9. Rc/Ra, $\delta^{13}C$–CO_2 and $\delta^{15}N$ versus longitude (DMS) for Hokkaido samples. Usu data (empty circle) are reported (Nagao et al., 1981; Giggenbach and Matsuo, 1991; Hernández et al., 2001) in order to support Tarumae data. The isotopic composition of Tokachi is very different from other volcanoes in Hokkaido. Empty symbols are for fumarole samples, "b" symbol is for bubbling gas sample and solid symbols are for hot spring samples. The gray field represents the estimated isotopic source for each volcano.

et al., 2010). Clift and Vannucchi (2004) estimated that the rate of material subduction is 93 km^3 $m.y^{-1}$ for the Kurile margin, and 155 km^3 $m.y^{-1}$ for the NE Honshu margin. They estimated a total subducted sediment contribution of 20% for Kurile and 23% for NE Honshu. Thus, increasing the volume of subducted sediments partially explains the variation of isotopic composition between Tarumae and Meakan in comparison with Tokachi.

(3) *Change in thermal regime*. The last hypothesis to completely explain the isotopic/geochemical variations in Hokkaido volcanoes is a change in the thermal regime. Ikeda et al. (1987) showed that Sr isotope ratios of volcanic rocks from the Kurile arc decrease from the volcanic front (Meakan; 0.7036) to the rear-arc (Rishiri; 0.7032), suggesting that the contribution of the subducted slab component becomes lower away from the volcanic front. This variation of Sr isotopes is also observed in volcanic rocks from Honshu arc (Notsu, 1983; from 0.7044 to 0.7033, respectively). The same variation is observed with K_2O contents. It is commonly accepted that K_2O contents in volcanic rocks increase from the volcanic front to rear-arc (from 1% to 2.5%, respectively; Katsui, 1961; Katsui et al., 1978; Nakagawa, 1992; Syracuse and Abers, 2006), related to a decrease of the degree of partial melting. Nakamura et al. (1985) explained such geochemical variations by the contamination of magmas by the fluid phase from dehydrated slab. More recent studies on subduction zones showed that variations of the isotopic and geochemical compositions are the result of a change in the thermal regime controlled by the subducting slab, depending on the shape, dip, and motion of the subducted plate, along with distance from the volcanic front (Iwamori, 1998; Hacker et al., 2003; Syracuse and Abers, 2006; Syracuse et al., 2010). Kurima and Yoshida (2006) reported deep mantle structure and schematic model of magma genesis in North Honshu in order to explain the geochemical/isotopical composition variations between volcanic front and rear arc volcanoes. Their model summarizes previous studies and shows the importance of the variation in terms of the sediment slab contribution, the degree of partial melting, and the proportion of dehydration slab. Syracuse and Abers (2006) presented a vertical cross section of Vp–Vs structure in Central America and Indonesia, and showed that the slab depth varies by tens of kilometers over short distances (<200 km) within arc segments. This jump appears to be formed at the end of the volcanic line, related to changes in the slab shape. This change is also correlated with the variations of geochemical proxies for melting process as K_2O. This observation has an important consequence on magma generation and caused the shift of the volcanic front related to the increase of the slab dehydration depth (up to 200 km). Wang and Zhao (2005), reported a vertical cross section of Vp and Vs in Northern Japan and Hokkaido. This study shows two main observations: the dip of the slab increases from Northern Japan to Hokkaido; and because the Tokachi volcano is located ~50 km behind the volcanic front, the dehydration of the slab occurs at depths between 150 km and 200 km. Meanwhile, for the Meakan and Tarumae volcanoes dehydration is estimated at a 100 km depth (Syracuse and Abers, 2006; Dreyer et al., 2010). Based on these observations, we suggest that the Tokachi volcano is located in a transitional zone, at the end of the Honshu arc and at the beginning of the Kurile arc, where a shift of the volcanic front occurs. Based on geochemical proxies (N, C, K_2O, and trace elements; Katsui et al., 1978), geophysical features (Wang and Zhao, 2005; Syracuse and Abers, 2006; Syracuse et al., 2010) and the calculation model of Kurima and Yoshida (2006), we suggest that Tokachi magmas are the result of a lower sediment contribution from the slab (lower than 3% based on Sr isotope ratios; Ikeda et al., 1987), a deeper dehydration of the slab (150–200 km under pressures of 5.5–6GPa), and a lower degree of partial melting (2–3% based on trace element patterns) related to the variation of the slab shape, which triggered a shift of the volcanic front.

6. Conclusions

Our new isotopic and geochemical data from the Tarumae, Tokachi, and Meakan (Hokkaido) hydrothermal fluids demonstrate that:

(1) Tokachi and Meakan hydrothermal fluid isotopic features correlate with the distance from the crater that is consistent with crustal contamination by host rocks.
(2) The magmatic signature from Tarumae fumaroles is affected by hydrothermal–crustal interaction (^4He and CO_2 addition) from aquifer and meteoric water penetration through the factures of the dome, or from deeper hydrothermal systems, that decrease the $^3He/^4He$ ratio to around 3R and increase $CO_2/^3He$ ratios.
(3) Olivine from Tarumae pumice (AD 1739) reflects a $^3He/^4He$ magmatic signature (5.22Ra), while cogenetic pyroxene shows radiogenic ^4He addition from late crust contamination (decreasing $^3He/^4He$ ratio to 3.73Ra).
(4) The isotopic magmatic source for Tarumae, Tokachi and Meakan are distinct, and show geographic variation along the volcanic front.
(5) Tokachi volcano has the lowest $\delta^{15}N$ (−2.4‰–+0.1‰) and $CO_2/^3He$ (2.12×10^9) values, and the highest Rc/Ra (7.5Ra) and $\delta^{13}C$–CO_2 (−5.29‰), consistent with a minor subducted sediment contribution compared to Tarumae and Meakan volcanoes.
(6) Tokachi volcano, located behind the volcanic front, is the result of changes in the direction of the slab at the end of the Honshu arc and the beginning of the Kurile arc. This change produces the rapid lateral change in dip of the subduction zone and a change in the slab shape. Hence, slab dehydration under Tokachi occurs at a deeper level than in other volcanoes in Hokkaido (150–200 km), inducing a shift of the volcanic front. Therefore, the isotopic signature of Tokachi is the result of (i) a lower sediment contribution from the slab, (ii) a deeper dehydration of the slab, and (iii) a lower degree of partial melting.

Acknowledgments

We thank the anonymous reviewers and the editor David Hilton for their thoughtful reviews. We wish to thank K. Kazahaya and M. Ohwada for their help during fieldwork. We thank Fernando Barra and Lucy McGee for English revision of an earlier version of the manuscript. E. Roulleau's research was funded through JSPS grant no. P11713 and CONICYT/FONDECYT grant no. 11130351.

References

Anderson, S.W., Fink, J.H., 1989. Hydrogen-isotope evidence for extrusion mechanisms of the Mount St Helens lava dome. Nature 341, 521–523.
Aramaki, S., 1984. Formation of the Aira Caldera, Southern Kyushu, 22,000 years ago. J. Geophys. Res. 89 (B10), 8485–8501.
Barry, P.H., et al., 2013. Helium and carbon isotope systematics of cold "Mazuku" CO_2 vents and hydrothermal gases and fluids from Rungwe Volcanic Province, southern Tanzania. Chem. Geol. 339, 141–156.
Calvache, M.L., Williams, S.N., 1997. Emplacement and petrological evolution of the andesitic dome of Galeras volcano, 1990–1992. J. Volcanol. Geotherm. Res. 77, 57–69.
Casadevall, T., et al., 1983. Gas emissions and the eruptions of Mount St. Helens through 1982. Science 221, 1383–1385.
Clift, P.D., Vannucchi, P., 2004. Controls on tectonic accretion versus erosion in subduction zones: Implications for the origin and recycling of the continental crust. Rev. Geophys. Space Phys. 42 (RG2001).
Clor, L.E., Fischer, T.P., Hilton, D.R., Sharp, Z.D., Hartono, U., 2005. Volatile and N isotope chemistry of the Molucca Sea collision zone: tracing source components along the Sangihe Arc, Indonesia. Geochem. Geophys. Geosyst. 6 (3), Q03J14.
Craig, H., Lupton, J.E., Horibe, Y., 1978. A mantle helium component in Circum-Pacific volcanic gases: Hakone, the Marianas, and Mr. Lassen. In: Alexander, E.C., Ozima, M. (Eds.), Advances in Earth and Planetary ScienceTerrestrial rare Gases. Academic publication, Japan, pp. 3–16.
Danyushevsky, L.V., Leslie, R.A., Crawford, A.J., Durance, P., 2004. Melt inclusions in primitive olivine phenocrysts: the role of localized reaction processes in the origin of anomalous compositions. J. Petrol. 45, 2531–2553.

Dodson, M.H., 1973. Closure temperature in cooling geochronological and petrological systems. Contrib. Mineral. Petrol. 40, 259–274.
Doi, S., 1957. Geology of the Tarumai-san district. Quadrangle Series, scale 1:50,000. Geological survey of Hokkaido: 51.
Dreyer, B.M., Morris, J.D., Gill, J.B., 2010. Incorporation of Subducted Slab-derived Sediment and Fluid in Arc Magmas: B–Be–10Be–dNd Systematics of the Kurile Convergent Margin, Russia. J. Petrol. 51 (8), 1761–1782.
Elkins, L.J., et al., 2006. Tracing nitrogen in volcanic and geothermal volatiles from the Nicaraguan volcanic front. Geochim. Cosmochim. Acta 70 (20), 5215–5235.
Finizola, A., et al., 2002. Fluid circulation at Stromboli volcano (Aeolian Islands, Italy) from self-potential and CO_2 surveys. J. Volcanol. Geotherm. Res. 116, 1–18.
Fink, J.H., Malin, M.C., Anderson, S.W., 1990. Intrusive and extrusive growth of the Mount St Helens lava dome. Nature 348, 435–437.
Fischer, T.P., et al., 2002. Subduction and recycling of nitrogen along the Central American margin. Science 297, 1154–1157.
Fischer, T., Takahata, N., Sano, Y., Sumino, H., Hilton, D.R., 2005. Nitrogen isotopes of the mantle: insights from mineral separates. Geophys. Res. Lett. 32. http://dx.doi.org/10.1029/2005GL022792.
Fischer, T.P.B., P., Marty, B., Hilton, D.R., Furi, E., Palhol, F., Sharp, Z.D., Mangasini, F., 2009. Upper-mantle volatile chemistry at Oldoinyo Lengai volcano and the origin of carbonatites. Nature 459 (7243), 77–80.
Fourre, E., Le Guern, F., Jean-Baptiste, P., 2002. Helium isotopes at Satsuma–Iwojima volcano, Japan. Geochem. J. 36, 493–502.
Gautheron, C., Moreira, M., 2002. Helium signature of the subcontinental lithospheric mantle. Earth Planet. Sci. Lett. 199 (1-2), 39–47.
Giggenbach, W.F., 1992a. The composition of gases in geothermal and volcanic systems as a function of tectonic setting. In: Y. K., Maest, K.a.A. (Eds.), Water Rock Interaction. A. A. Balkema, Brookfield, Vt., pp. 873–878.
Giggenbach, W.F., 1992b. The composition of gases in geothermal and volcanic systems as a function of tectonic setting. In: Maest, Y.K.K.a.A.S. (Ed.), Water–Rock, Interaction, pp. 873–878.
Giggenbach, W.F., Corrales, S.R., 1992. Isotopic and chemical composition of water and steam discharges from volcanic–magmatic–hydrothermal systems of the Guanacaste Geothermal Province, Costa Rica. Appl. Geochem. 7 (4), 309–332.
Giggenbach, W.F., Glover, R.B., 1992. Tectonic regime and major processes governing the chemistry of water and gas discharges from the rotorua geothermal field, New Zealand. Geothermics 21 (1–2), 121–140.
Giggenbach, W.F., Goguel, R.L., 1989. Collection and Analysis of Geothermal and Volcanic Water and Gas Discharges. DSIR Chemistry, Report 2401.
Giggenbach, W.F., Matsuo, S., 1991. Evaluation of results from Second and Third IAVCEI Field Workshops on Volcanic Gases, Mt Usu, Japan, and White Island, New Zealand. Appl. Geochem. 6 (2), 125–141.
Giggenbach, W.F., Poreda, R.J., 1993. Helium isotopic and chemical composition of gases from volcanic–hydrothermal systems in the Philippines. Geothermics 22, 369–380.
Giggenbach, W.F., Sano, Y., Wakita, H., 1993. Isotopic composition of helium, and CO_2 and CH_4 contents in gases produced along the New Zealand part of a convergent plate boundary. Geochim. Cosmochim. Acta 57 (14), 3427–3455.
Graham, D.W., 2002. Noble gas isotope geochemistry of mid-ocean ridge and ocean island basalts: characterization of mantle source reservoirs. Rev. Mineral. Geochem. 47 (1), 247–317.
Hacker, B.R., Peacock, S.M., Abers, G.A., Holloway, S.D., 2003. Subduction factory: 2. are intermediate-depth earthquakes in subducting slabs linked to metamorphic dehydration reactions? J. Geophys. Res. 108 (B1).
Halldorsson, S.A., Hilton, D.R., Troll, V.R., Fischer, T.P., 2013. Resolving volatile sources along the western Sunda arc, Indonesia. Chem. Geol. 339, 263–282.
Harrison, D., Barry, T., Turner, G., 2004. Possible diffusive fractionation of helium isotopes in olivine and clinopyroxene phenocrysts. Eur. J. Mineral. 16, 213–220.
Heki, K., Mitsui, Y., 2013. Accelerated pacific plate subduction following interplate thrust earthquakes at the Japan trench. Earth Planet. Sci. Lett. 363, 44–49.
Hernández, P.A., et al., 2001. Carbon dioxide degassing by advective flow from Usu Volcano, Japan. Science 292 (83–86).
Hernandez, P.A., et al., 2001a. Diffuse emission of CO_2 from Miyakejima volcano, Japan. Chem. Geol. 177 (12), 175–185.
Hernandez, P.A., et al., 2001b. Preliminary results of diffuse emissions of CO_2 and soil gas pressure gradient measurements at Tarumae volcano, Japan. Bull. Volcanol. Soc. Jpn. 46, 121–125.
Hilton, D.R., Craig, H., 1989. A helium isotope transect along the Indonesian archipelago. Nature 342, 906–908.
Hilton, D., Hoogewerff, J., van Bergen, M., Hammerschmidt, K., 1992. Mapping magma sources in the east Sunda-Banda arcs, Indonesia: constraints from helium isotopes. Geochim. Cosmochim. Acta 56, 851–859.
Hilton, D.R., Barling, J., Wheller, G.E., 1995. Effect of shallow-level contamination on the helium isotope systematics of ocean-island lavas. Nature 373, 330–333.
Hilton, D.R., McMurtry, G.M., Goff, F., 1998. Large variations in vent fluid $CO_2/^3He$ ratios signal rapid changes in magma chemistry at Loihi Seamount, Hawaii. Nature 396, 359–362.
Hilton, D.R., Fischer, T.P., Marty, B., 2002. Noble gases and volatile recycling at subduction zones. In: R.i.M.a. Geochemistry (Ed.), Noble Gases in Geochemistry and Cosmochemistry, pp. 319–370.
Hoefs, J., 2009. Stable Isotope Geochemistry (288 pp.).
Ichihara, H., Mogi, T., Yamaya, Y., 2013. Three-dimensional resistivity modelling of a seismogenic area in an oblique subduction zone in the western Kurile arc: constraints from anomalous magnetotelluric phases. Tectonophysics 603, 114–122.
Ikeda, Y., Katsui, Y., Kurasawa, H., 1987. Origin of lateral variations in $^{87}Sr/^{86}Sr$ ratios of Quaternary volcanic rocks from the Kurile arc in Hokkaido, Japan. J. Fac. Sci. Hokkaido Univ. Ser. 4 22 (2), 325–335.
Inguaggiato, S., Rizzo, A., 2004. Dissolved helium isotope ratios in ground-waters: a new technique based on gas–water re-equilibration and its application to Stromboli volcanic system. Appl. Geochem. 19, 665–673.
Iwamori, H., 1998. Transportation of H_2O and melting in subduction zones. Earth Planet. Sci. Lett. 160, 65–80.
Jaffe, L.A., Hilton, D.R., Fischer, T.P., Hartono, U., 2004. Tracing magma sources in an arc–arc collision zone: helium and carbon isotope and relative abundance systematics of the Sangihe Arc, Indonesia. Geochem. Geophys. Geosyst. 5 (4), Q04J10.
Japan Meteorological Agency, 2005. National Catalogue of the Active Volcanoes in Japan, (in Japanese).
JMA, 2012. Monthly Volcanic Activity Report.
Katsui, Y., 1961. Petrochemistry of the Quaternary volcanic rocks of Hokkaido and surrounding areas. J. Fac. Sci. Hokkaido Univ. Ser. 4 11, 1–58.
Katsui, Y., et al., 1978. Petrochemistry of the Quaternary volcanic rocks of Hokkaido, North Japan. J. Fac. Sci. Hokkaido Univ. Ser. 4 18, 449–484.
Katsumata, K., Wada, N., Kasahara, M., 2003. Newly imaged shape of the deep seismic zone within the subducting Pacific plate beneath the Hokkaidocorner, Japan–Kurile arc–arc junction. J. Geophys. Res. Atmos. 108 (B12, 2565).
Kita, I., Nitta, K., Nagao, K., Taguchi, S., Koga, A., 1993. Difference in N_2/Ar ratio of magmatic gases from northeast and southwest Japan: New evidence for different states of plate subduction. Geology 21, 391–394.
Kurima, J.-I., Yoshida, T., 2006. Contributions of Slab Fluid, Mantle Wedge and Crust to the Origin of Quaternary Lavas in the NE Japan Arc. J. Petrol. 47 (11), 2185–2232.
Mabry, J., Lan, T., Burnard, P., Marty, B., 2013. High-precision helium isotope measurements in air. J. Anal. At. Spectrom. 28 (12), 1903–1910.
Marty, B., 1995. Nitrogen content of the mantle inferred from N_2-Ar correlation in oceanic basalts. Nature 377, 326–329.
Marty, B., Dauphas, N., 2003. The nitrogen record of crust–mantle interaction and mantle convection from Archean to Present. Earth Planet. Sci. Lett. 206, 397–410.
Marty, B., Tolstikhin, I.N., 1998. CO_2 fluxes from mid ocean ridges, arcs and plumes. Chem. Geol. 145, 233–248.
Marty, B., Zimmermann, L., 1999. Volatiles (He, C, N, Ar) in mid-ocean ridge basalts: assessment of shallow-level fractionation and characterization of source composition. Geochim. Cosmochim. Acta 63 (21), 3619–3633.
Marty, B., Jambon, A., Sano, Y., 1989. Helium isotopes and CO_2 in volcanic gases of Japan. Chem. Geol. 76 (1–2), 25–40.
Mori, T., et al., 2006. Sulfur dioxide fluxes from the volcanoes of Hokkaido, Japan. J. Volcanol. Geotherm. Res. 158, 235–243.
Nagao, K., Takaoka, N., Matsubayashi, O., 1981. Rare gas isotopic compositions in natural gases of Japan. Earth Planet. Sci. Lett. 53 (2), 175–188.
Nakagawa, M., 1992. Spatial variation in chemical composition of Pliocene and Quaternary volcanic rocks in southwestern and Quaternary volcanic rocks in southwestern Hokkaido, Northeastern Japan Arc. J. Fac. Sci. Hokkaido Univ. Ser. 4 Geol. Mineral. 23 (2), 175–197.
Nakamura, E., Campbell, I.H., Sun, S., 1985. The influence of subduction processes on the geochemistry of Japanese alkaline basalts. Nature 316, 55–58.
Notsu, K., 1983. Strontium isotope compost ion in volcanic rocks from the Northeast Japan arc. J. Volcanol. Geotherm. Res. 18, 531–548.
Ozima, M., Podosek, F.A., 2002. Noble Gas Geochemistry. Cambridge University Press (300 pp.).
Poreda, R., Craig, H., 1989. Helium isotope ratios in circum-Pacific volcanic arcs. Nature 338 (6215), 473–478.
Ray, M.C., Hilton, D.R., Munoz, J., Fischer, T.P., Shaw, A.M., 2009. The effects of volatile recycling, degassing and crustal contamination on the helium and carbon geochemistry of hydrothermal fluids from the Southern Volcanic Zone of Chile. Chem. Geol. 266 (1-2), 38–49.
Roulleau, E., Sano, Y., Takahata, N., Kawagucci, S., Takahashi, H., 2013. Volatile isotopes and fluxes in Aira caldera: evidence for a common magmatic source with different degassing activities for both Sakurajima volcano and Wakamiko crater, Kyushu, Japan. J. Volcanol. Geotherm. Res. 258, 163–175.
Sano, Y., Marty, B., 1995. Origin of carbon in fumarolic gas from island arcs. Chem. Geol. 119 (1–4), 265–274.
Sano, Y., Wakita, H., 1985. Geographical distribution of $^3He/^4He$ ratios in Japan: implications for arc tectonics and incipient magmatism. J. Geophys. Res. 90 (B10), 8729–8741.
Sano, Y., Wakita, H., 1988. Helium isotope ratio and heat discharge rate in the Hokkaido Island, Northeast Japan. Geochem. J. 22, 293–303.
Sano, Y., Williams, S.N., 1996. Fluxes of mantle and subducted carbon along convergent plate boundaries. Geophys. Res. Lett. 23 (20), 2749–2752.
Sano, Y., Hirabayashi, J.-I., Oba, T., Gamo, T., 1994. Carbon and helium isotopic ratios at Kusatsu-Shirane Volcano, Japan. Appl. Geochem. 9 (4), 371–377.
Sano, Y., Takahata, N., Nishio, Y., Marty, B., 1998a. Nitrogen recycling in subduction zones. Geophys. Res. Lett. 25 (13), 2289–2292.
Sano, Y., Nishio, Y., Sasaki, S., Gamo, T., Nagao, K., 1998b. Helium and carbon isotope systematics at Ontake volcano, Japan. J. Geophys. Res. 103 (B10), 23, 863–23, 873.
Sano, Y., Takahata, N., Nishio, Y., Fischer, T.P., Williams, S.N., 2001. Volcanic flux of nitrogen from the Earth. Chem. Geol. 171 (3–4), 263–271.
Sano, Y., Takahata, N., Seno, T., 2006. Geographical distribution of $^3He/^4He$ ratios in the Chugoku district, Southwestern Japan. Pure Appl. Geophys. 163, 745–757.
Sano, Y., Tokutake, T., Takahata, N., 2008. Accurate measurement of atmospheric helium isotopes. Anal. Sci. 24 (4), 521–525.
Sato, M., Mori, T., Notsu, K., Wakira, H., 1999. Carbon and helium isotopic composition of fumarolic gas and hot spring gases from Kirishima volcanic area. Volcanol. Soc. Jpn. 6, 279–283.
Sato, M., Mori, T., Shimoike, Y., Nagao, K., Notsu, K., 2002. Carbon isotope systematics of CO_2, CO and CH_4 in fumarolic gases from Satsuma-Iwojima volcanic island, Japan. Earth Planets Space 54, 257–263.

Scott, J., Kusakabe, M., Hirabayashi, J., Ohba, T., Nagao, K., 1994. Geochemical evolution and origin of volcanic gases and springs in Japan. J. Geol. Soc. Philipp. 49, 89–110.
Shaw, A.M., Hilton, D.R., Fischer, T.P., Walker, J.A., Alvarado, G.E., 2003. Contrasting He–C relationships in Nicaragua and Costa Rica: insights into C cycling through subduction zones. Earth Planet. Sci. Lett. 214 (3–4), 499–513.
Shaw, A.M., Hilton, D.R., Fischer, T.P., Walker, J.A., de Leeuw, G.A.M., 2006. Helium isotope variations in mineral separates from Costa Rica and Nicaragua: assessing crustal contributions, timescale variations and diffusion-related mechanisms. Chem. Geol. 230 (1-2), 124–139.
Shinohara, H., 2005. A new technique to estimate volcanic gas composition: plume measurements with a portable multi-sensor system. J. Volcanol. Geotherm. Res. 143, 319–333.
Snyder, G., Poreda, R., Hunt, A., Fehn, U., 2001. Regional variations in volatile composition: Isotopic evidence for carbonate recycling in the Central American volcanic arc. Geochem. Geophys. Geosyst. 2.
Syracuse, E.M., Abers, G.A., 2006. Global compilation of variations in slab depth beneath arc volcanoes and implications. Geochem. Geophys. Geosyst. 7 (5), Q05017.
Syracuse, E.M., van Keken, P.E., Abers, G.A., 2010. The global range of subduction zone thermal models. Phys. Earth Planet. Inter. 183 (1–2), 73–90.
Takahata, N., Nishio, Y., Yoshida, N., Sano, Y., 1998. Precise isotopic measurements of nitrogen at the sub-nanomole level. Anal. Sci. 14, 485–491.
Taran, Y., 2011. N2, Ar, and He as a tool for discriminating sources of volcanic fluids with application to Vulcano, Italy. Bull. Volcanol. 73 (4), 395–408.
Trull, T.W., Kurz, M.D., 1993. Experimental measurements of 3He and 4He mobility in olivine and clinopyroxene at magmatic temperatures. Geochim. Cosmochim. Acta 57 (6), 1313–1324.
van Soest, M.C., Hilton, D.R., Macpherson, C.G., Mattey, D.P., 2002. Resolving sediment subduction and crustal contamination in the Lesser Antilles island Arc: a combined He–O–Sr isotope approach. J. Petrol. 43, 143–170.
von Huene, R., Arthur, M.A., 1982. Sedimentation across the Japan Trench off northern Honshu Island. Geol. Soc. Lond., Spec. Publ. 10 (1), 27–48.
Wang, Z., Zhao, D., 2005. Seismic imaging of the entire arc of Tohoku and Hokkaido in Japan using P-wave, S-wave and sP depth-phase data. Phys. Earth Planet. Inter. 152 (3), 144–162.
Watanabe, Y., 1993. Late Cenozoic stress field in northern part of southwest Hokkaido based on trends of dikes and craters. J. Geol. Soc. Jpn. 99, 105–116.
Yamaya, Y., Mogi, T., Hashimoto, T., Ichihara, H., 2009. Hydrothermal system beneath the crater of Tarumai volcano, Japan: 3-D resistivity structure revealed using audio-magnetotellurics and induction vector. J. Volcanol. Geotherm. Res. 187, 193–202.
Zimmer, M.F., T.P., Hilton, D., Alvarado, G., Sharp, Z., Walker, J., 2004. Nitrogen systematics and gas fluxes of subduction zones: Insights from Costa Rica arc volatiles. Geochem. Geophys. Geosyst. 5 (5).